Aeroacoustic Flight Test Data Analysis and Guidelines for Noise-Abatement-Procedure Design and Piloting

Pierre Spiegel[1], Frédéric Guntzer[1], Anne Le Duc[1], Heino Buchholz[1]
[1] DLR : Deutsches Zentrum für Luft und Raumfahrt e.V. in der Helmholtz-Gemeinschaft,
Institute of Aerodynamics and Flow Technology, Technical Acoustics Division,
Lilienthalplatz 7, 38108 Braunschweig, Germany
www.dlr.de
(corresponding author: Pierre.Spiegel@dlr.de)

Abstract: This paper focuses on noise abatement flight procedure (NAFP) studies performed on an EC135 helicopter. Aeroacoustic flight tests performed in the framework of the DLR PAVE project have been analyzed in order to provide guidance for NAFP design. Flyability limits and noise sensitivity to main control parameters have been investigated in simulator and in flight in order to improve the NAFP design and optimization and to develop dedicated pilot displays. The torque appears to be a parameter governig the blade-vortex interaction (BVI) noise: piloting at very low torque or at high torque allows to avoid BVI noise. Thus, the engine torque display, available on almost all helicopters, can be used to avoid BVI conditions. It was also found that the very annoying Fenestron noise excess that appears when flying with low torque to avoid BVI, can be completely eliminated through side-slip. NAFP validation flight tests for the PAVE and Friendcopter projects are briefly presented. Examples of NAFP resulting in measured noise reductions close to 10 dB SEL are provided. A guideline to pilots explains how to perform quietly an EC135 complete landing approach with almost no BVI noise, no Fenestron excess noise, and possibly using only instruments commonly on board.

Notation

A complete list of all variables relating to helicopter aerodynamics and acoustics with exhaustive definition can be found on "www.dlr.de/as/Friendcopter-dictionary". We list here the principal variables and abbreviations used in this article.

Name	Symbol	Signification
beta	β	Side slip angle
gammaA	γ_a	Air-path climb angle
phi	ϕ	Roll (or bank) angle
PmAlpha	α_{Pm}	Tip path plane angle of attack (for main rotor)
psi	ψ	Heading angle
RmCT	CT_{Rm}	Main rotor thrust coefficient
RmMu	μ_{Rm}	Main rotor advance ratio
theta	θ	Pitch angle

Presented at the 34th European Rotorcraft Forum, 16th – 19th September 2008, Liverpool, UK.

BVI	:	Blade Vortex Interaction
FHS	:	Flying Helicopter Simulator
MR	:	Main Rotor
NAFP	:	Noise Abatement Flight Procedure

Fig. 1. EC135-FHS performing a flare with side-slip at Magdeburg-Cochstedt Airport during 2008 flight tests of noise abatement procedures.

INTRODUCTION

The paper presents flight test results and methods for designing and flying **N**oise **A**batement **F**light **P**rocedures (NAFP).

Because of the increasing air traffic and the enhanced public sensitivity to noise annoyance, the rotorcraft industry and operators are faced with demands on noise reduction. New rotorcraft design can reduce noise emission, for instance with improved passive elements, or with additional active control systems (on rotor blade pitch, blade flaps, blade twist…). For existing (and new) rotorcraft models, the noise perceived on the ground can also be minimized through NAFP. Here we focus on this second approach.

DLR has been working on this approach since 2000 [1], particularly since 2002 in the framework of the DLR internal project PAVE (Pilot Assistant in the Vicinity of hElipads) [2-5] and since 2004 in the framework of the European Project Friendcopter, Work Package 2 “Noise Abatement Procedures”. In 2004, aeroacoustic flight tests were performed in PAVE for gathering noise directivities all over the flight envelope, including for maneuver flights, on the DLR test helicopters BO105 and EC135 FHS [6]. We focus in this paper only on the EC135-FHS results and noise abatement procedures. In Friendcopter as well as in PAVE, DLR’s goal was to design noise abatement procedures using the acquired experimental data base, however with different methods. In PAVE the goal was to use engineering understanding of the noise emission parameters as for example presented in [7], whereas in Friendcopter an optimization process was implemented in order to find the maximum noise reduction achievable through flight procedures satisfying flyability and safety aspects. The computational chain used within the optimization loop is presented in [8] (but not the optimization itself). Both projects include the design of pilot displays. In PAVE, a multi-purpose display enabling in-flight mission replanning, navigation, 3D visualization of landing site, flight in low visibility, following of noise abatement procedures has been developed. In Friendcopter, the unique objective of the pilot display was to help pilots to follow accurately the optimized noise abatement procedures in order to validate them during acoustic flight tests. For this second display, specific methods could be developed, as for example the avoidance of noisy path corrections when discrepancies with the prescribed path occur.

This paper is organized as follows. It first presents data documentation and storage techniques applied to the 2004 PAVE flight tests in the framework of a general data harmonization process (Section 1). In Section 2, examples of data reduction showing some noise trends are provided. In Section 3, it is explained how flyability tests performed in flight during the noise abatement procedure design phase led to improved flyability criteria for the automatic noise footprint minimization process, and to requirements for the pilot displays. The experienced and understanding gained in these preliminary tests (all meant to prepare the validation flight tests) lead to new ideas and ways to perform landing approaches with less device assistance. Section 4 explains how the main rotor torque or the engine torque (displayed in all helicopters) was found to be a reliable BVI noise indicator. Section 5 presents briefly the validation flight tests performed in 2008 (Fig. 1). Examples of results are used in the following sections. Section 6 explains how Fenestron excess noise could be avoided once BVI noise is avoided. The derived ways to fly quietly are explained in Section 7 and validated with flight test results. In particular, a way to perform a complete landing approach with almost no BVI noise and without Fenestron noise excess is shown as guideline to pilots. It can be realized without a sophisticated display.

The automatic noise footprint optimization performed in Friendcopter before the validation flight tests as well as the validation flight tests themselves and the Friendcopter Display development will be presented in details in future publications.

In order to consider manufacturer interest to keep some helicopter characteristics confidential, the noise results shown in this paper are all amplified by a factor, the same over the whole paper.

Coordinate systems (3 out of 22)

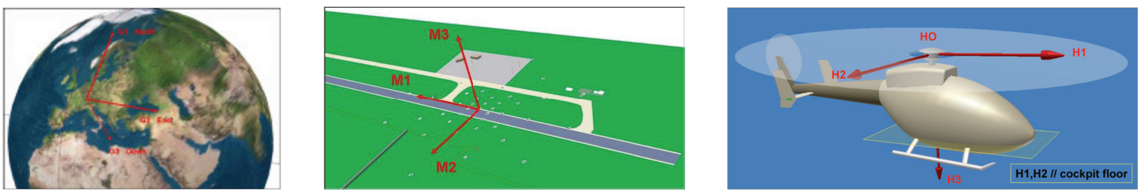

G: Ground CS | M: Microphone CS | H: Aircraft CS

Variables (1 out of 400)

Name : usable in source code

Variable/paragraph number

Name : usable in formulas

2.7.1 beta : β
Unit : deg
Def. : Side slip angle. is the angle of ***VAircraft_Air*** with respect to the symmetry plane of the aircraft , where ***VAircraft_Air*** is the velocity vector of the aircraft with respect to ambient air. Positive if the flow ***VAir_Aircraft*** comes on the Aircraft from starboard

Fig. 2. Example of coordinate systems and variables defined in the Friendcopter Dictionary.

1. DATA REDUCTION AND DOCUMENTING IN A STEP TOWARDS DATA HARMONIZATION

A dictionary describing coordinate systems and variables has been written in order to increase the efficiency and reliability of exchanges between the actors of flight tests, wind-tunnel tests and computational simulations. It covers the fields of flight mechanics, aerodynamics, acoustics, and atmospheric conditions and is usable as well for airplanes and tilt-rotors as for helicopters. Its focus is to provide exhaustive definitions of variables and coordinate systems. It represents the necessary first step in data harmonization. The dictionary has been started in the Friendcopter project Work Package 2 “Noise Abatement Procedures” and is still growing. It contains presently the definition of 22 coordinate systems and 400 variables. The dictionary, mainly written at DLR, has been adopted as a standard in the Friendcopter project WP2, for flight tests, and for collective development of the HELENA code. It is now available on request at "www.dlr.de/as/Friendcopter-dictionary".

The dictionary consists of a text pdf file and of a Microsoft Excel sheet allowing extension for translation between dictionary names and locally used names (in codes, data bases…). Rules for naming coordinate systems, and for naming variables are given at the begin of the pdf document. For example it has been decided to name coordinate systems as much as possible with a single letter, as for example E for the Earth coordinate system. The origin of this system is then named EO and the vectors of the associated right handed base are named E1, E2, E3. The choice to name coordinate systems as shortly as possible was made in order to refer to coordinate systems in variable names without generating long names. For example, the variable VP_HE1 is the first (“1”) component in the Earth coordinate system “E” of the velocity (“V”) of point “P”, fixed in the aircraft coordinate system “H”, with respect to E. There is also a general rule for naming the variables so that when reading it from left to right, one passes from the more general concept to the more detailed aspects. For example, RmTorque, means the Torque of the main rotor Rm. RtBlaNum is the Number of Blades of the tail rotor Rt. Example of definitions are shown in Fig. 2. Each variable has a name usable in source codes, a name usable in formulas (often a symbol) and also a long name, or short explanation, in about 5 words used to recall the variable meaning. An exhaustive definition is associated to each name. The long names do not replace the definitions.

In Fig. 3 the upper left corner of the excel sheet is presented. The vertical structure is the same as in the pdf document. Title levels are highlighted in a series of colours. The coordinate systems are marked in light green lines. The left hand side of the table is write protected, and on the right hand side columns, users can write the translation to the local names used in their documents or codes, or mark the variables belonging to a file. When users write the translation between their local variables and the dictionary variables, they automatically get the translation to the variables of the other users, using the dictionary as common intermediate.

Common variable or symbol definition part, write protected, public domain								User field: local names (code, doc., files)			
								code LAMBDA			
Definition in paragraph	Variable or Coordinate System (CS) name	Variable or CS short description (or long name) (English)	Fren	German	Unit	Chronological Index (CI) Present Max 564		CI	Local index 0	Local variable/CS name if non common	Unit if non common
2		**EARTH BASED COORDINATE SYSTEMS** and related variables									
2.1	**E**	**Earth WGS84 CS**				127					
2.1.1	longitude	Longitude on WGS84 Earth ellipsoid			deg	1					
2.1.2	latitude	Latitude on WGS84 Earth ellipsoid			deg	2					
2.1.3	height	Height on WGS84 Earth ellipsoid			m	3					
3		**LOCAL TERRAIN COORDINATE SYSTEMS** and related variables									
3.1	**G**	**Ground CS : ground point, North, East, Down**				128					
3.1.1	psi_MagNorth	Azimuth of magnetic North (magnetic declination)			deg	160					
3.2	**M**	**Microphone CS**				129					
3.2.1	psiM	Main flight path direction wrt ground North			deg	4					
3.3	**N**	**Noise Footprint CS**				130					
3.3.1	dpsiN	Direction of a given flight wrt M1			deg	5					
3.4	**S**	**Simulation CS**				131					
3.4.1	psiS	Angle of S1 wrt Local North			deg	126					
4		**AIRCRAFT DESCRIPTION**									
4.1		**Aircraft general characteristics**									
4.1.1	AircraftName	Aircraft name			characters	150					
4.1.2	MTOMass	Maximum Take Off Mass			kg	101					
4.1.3	Vh	Maximal horizontal velocity			m/s	102					
4.1.4	Vy	Aircraft speed for maximal vertical velocity			m/s	103					
4.1.5	BRC	Best Rate of Climb			m/s	104					
4.2		**Fuselage**									
4.2.1	**H**	**Aircraft CS**				133					
4.2.1.1	H_ComplementDef	Complementary definition of H for a specific helicopter			char	320					
4.2.2	**D**	**Design CS (to describe the aircraft geometry)**				132					
4.2.2.1	D_ComplementDef	Complementary definition of D for a specific helicopter			char	182					
4.2.3	NGC_H1	Coordinate of Neutral Gravity Center along H1			m	58					
4.2.4	NGC_H2	Coordinate of Neutral Gravity Center along H2			m	59					
4.2.5	NGC_H3	Coordinate of Neutral Gravity Center along H3			m	60					
4.3		**Rotors (or propellers)**									
4.3.1	RNum	Number of rotors			int	189					
4.3.2	RNameList	Rotor name list, Rm(main), Rt(tail)…			characters	190					
4.3.3		**Generic rotor-x "Rx"**									

Fig. 3. View of the Excel file joined to the pdf Friendcopter dictionary. On the left hand side the variables and coordinate systems are listed. On the right hand side columns users can write the translation to their local names used in documents or codes, or mark the variables belonging to a file.

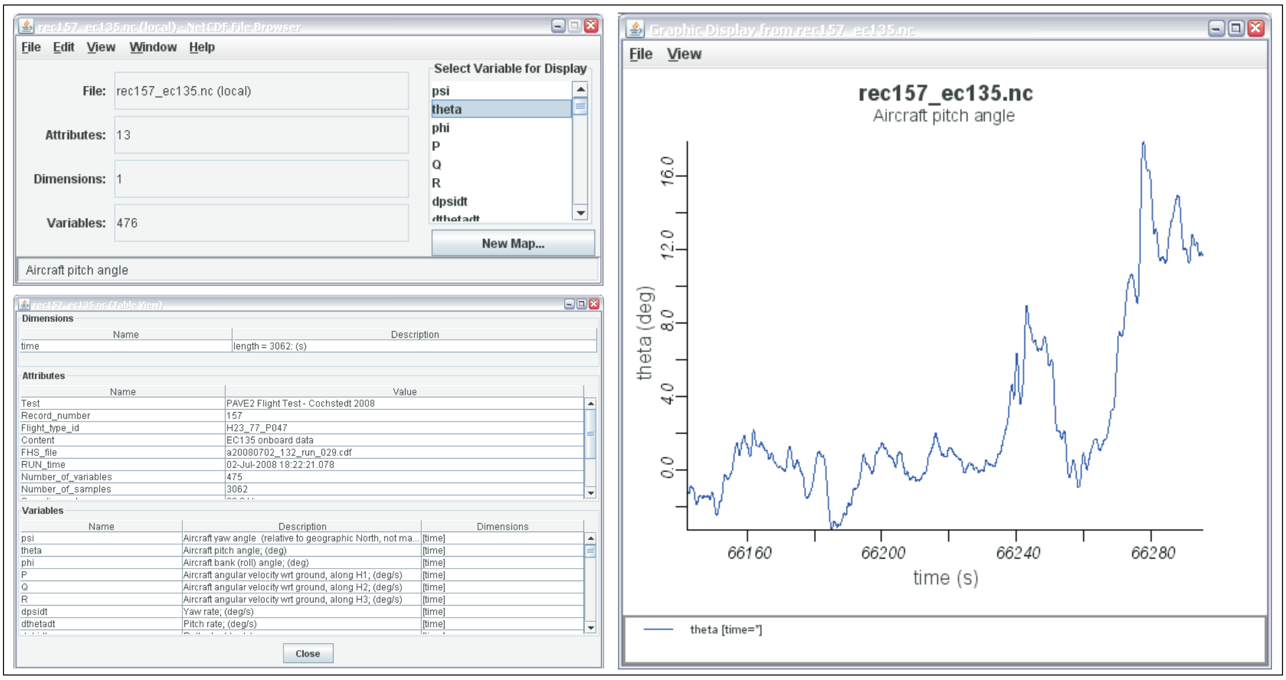

Fig. 4. Example of flight condition netCDF file visualization with ncBrowse.

The Excel file, with its sorting possibilities should facilitate updating the translation to local variables when the dictionary grows. A chronological index is used and the variables can either be sorted chronologically for updating works or according to the structure of the pdf document for daily use. An index, as well as many hyperlinks has been introduced in the pdf file for navigating easily in the document. Regarding the dictionary extension, proposals are made by partners. Other partners have then a given time to provide feed-back and final definitions are agreed and inserted in the dictionary. A particular effort is made to generate definitions identical with well established conventions or norms ([9], [10]). Sometimes only the variable name changes, in comparison to already existing definitions, in order to respect the naming conventions. For example the definitions of the coordinate systems G and H presented in Fig. 2 are not entirely new, and for the variable beta defined in the figure, even the current name has been kept.

The data of the PAVE flight tests of 2004 are formatted according to the two following requirements:

1 – All variables have to be defined in the Friendcopter Coordinate System and Variable Dictionary. The dictionary must be extended if needed.

2 – The netCDF format is used (compact, portable, fast access, easy to view, free) for data storage.

The flight test results of 2004 comprise the noise recorded on 43 ground microphones, the detailed flight conditions and path, and weather. 243 measurement runs (overflights) were performed with the EC135-FHS, and 110 flights with the BO105. The overflights covered maneuver flights as well as the steady-flight envelope, and the resulting definitions and netCDF files are proposed as common flight test data formatting for the Friendcopter tests on EC130, A109 and EC135.

An example of netCDF file visualization with the freeware ncBrowse is shown in Fig. 4.

2. NOISE TREND ANALYSES FROM FLIGHT TESTS

Once the flight test data base is formatted, the noise emission is analyzed with respect to flight conditions. Steady flights and maneuvering flights are considered. The microphone layout of the PAVE 2004 tests is recalled in Fig. 5. 43 microphones were scattered on an 800 m diameter disk, at the Magdeburg-Cochstedt Airport (Germany). A DLR wireless acoustic measurement system was used. The microphone layout is meant to provide a homogeneous angular distribution on directivity spheres obtained by back-propagating the noise measured on the microphones (see [6; 8]) when the helicopter horizontal distance to the central microphone is lower than 150 m. Note that for all the acoustic results shown in this section the ground microphone directivity effect illustrated in [6] (which can reach 10 dBA for the most grazing incidences) is not corrected here. The noise was measured with inverted ground microphones. The microphones located on grass were mounted on a 0.4 m diameter metal plate. Both flight directions were used in order to make the flight tests more efficient: the one indicated by the arrow in Fig. 5 and the opposite one.

In Fig. 6 the effect of the glide slope on EC135 noise footprints is shown for 65 kts flights. The top row of plots represents the dB SEL (Sound Exposure Level) levels measured during the flights. The row below is the instantaneous dBA footprint when the helicopter is above the central microphone. Even if the flights were meant to be steady the true flight conditions varied slightly due to turbulence or pilot corrections. The slope indicated in the figure is the aerodynamic slope gammaA when the helicopter is over the central microphone. What is called dBA max on the figure is the highest dBA level observed on the instantaneous noise footprint (snapshot) at this time (when the helicopter is above the central microphone). The height measured by

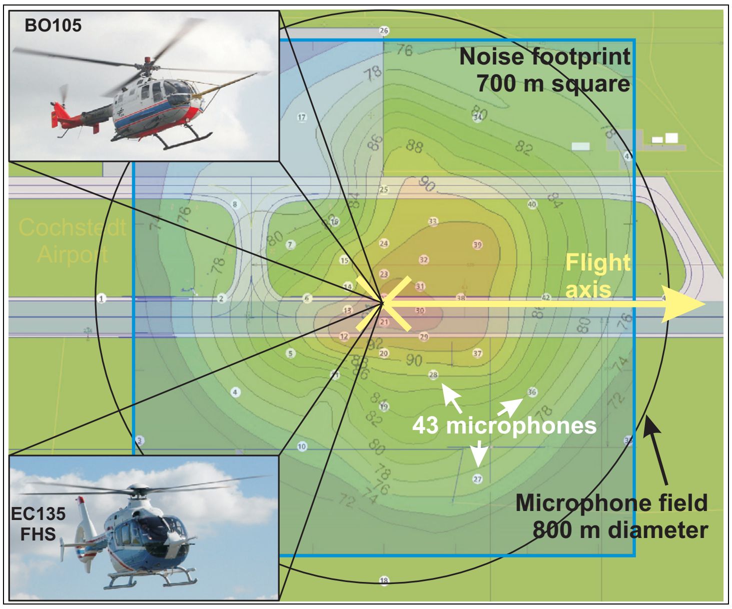

Fig. 5. Microphone layout during the PAVE 2004 tests and view of the noise footprint size used in the following figures.

radar altitude, which varied between 78 m and 98 m at this time, for the selected cases, was used to correct the dBA max value to a common height of 100 m in the dBAmax versus gammaA plot. One can notice that the noise level is largest for gammaA between 3 and 12 degrees. This is attributed to main rotor BVI noise. At 13 degrees, the noise is smaller, which is attributed to BVI noise alleviation through convection of the vortices above the main rotor. For angles higher than 15 degrees the noise footprint becomes larger again. This effect, clearly audible, is attributed to Fenestron noise whose operating conditions are changed. Indeed, in steep descent, the main rotor is close to autorotation and no anti-torque effort is needed from the tail boom. The profiled vertical tail planes nevertheless generate a lateral force due to their pre-build angle of attack and the Fenestron has then to compensate for it through inverse flow. This results in the ingestion of the stator wake by the rotor, which is known as a noisy configuration. The noise increase does not appear on the lower plot which considers only the maximum dBA level. In summary, to fly descent at 65 kts with low BVI noise and low Fenestron noise, there are only two possibilities: gammaA higher than -2 degrees (only 1.2 m/s sink rate, not efficient) or gammaA between -12 and -15 degrees. Note that, as shown in [6], for the BO105 with conventional tail rotor, the noise continues to decrease when the slope becomes steeper than gammaA = 15 deg. This tends to indicate that the noise of the main rotor of the EC135 continues to decrease with larger descent slopes and this could benefit to the overall noise reduction when the Fenestron noise excess is eliminated.

In Fig. 7, the EC135 footprint evolution in horizontal flight is shown, first as function of velocity in steady flight (top footprints), then as function of acceleration in

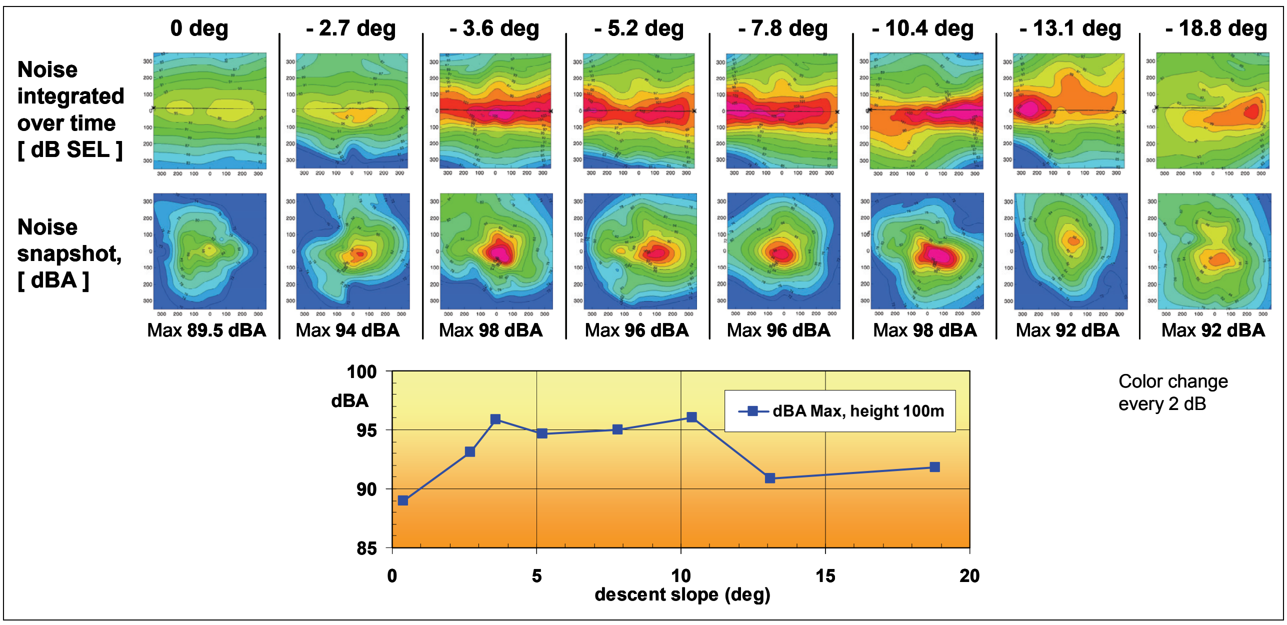

Fig. 6. Evolution of the noise footprint of EC135 at 65 knots versus path slope.

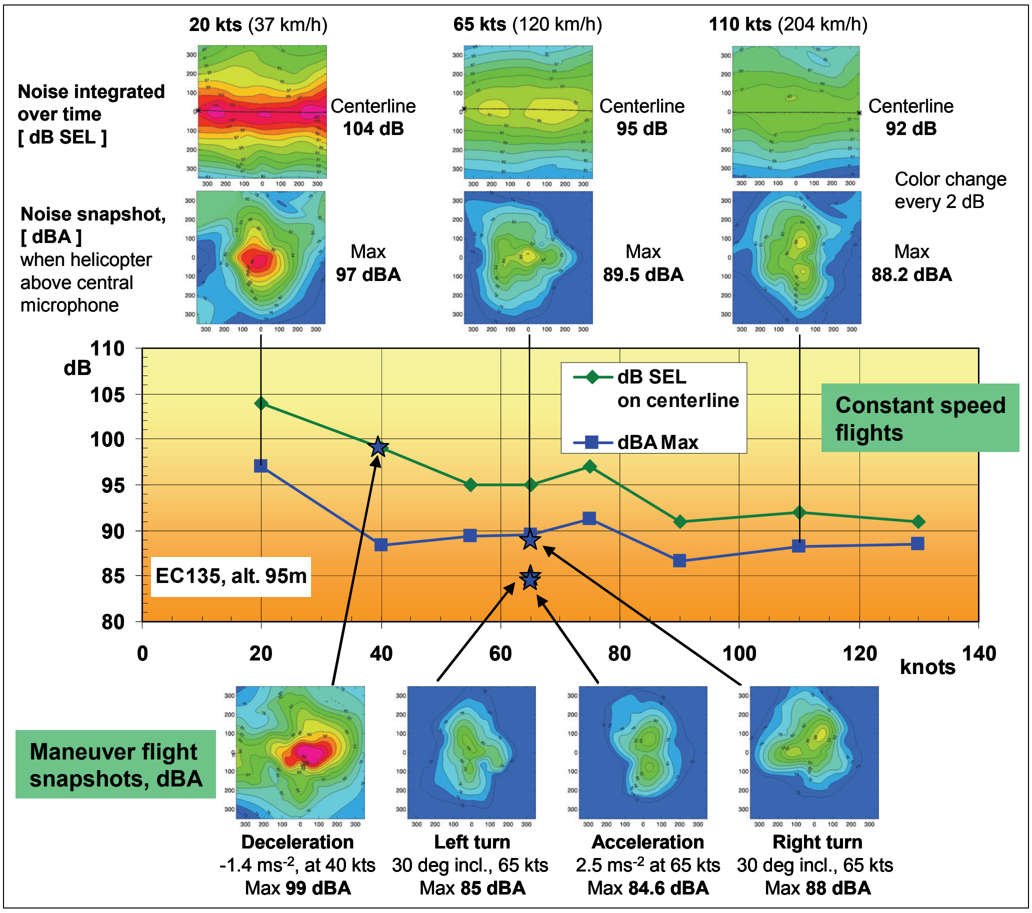

Fig. 7. Evolution of the noise footprint of EC135 at horizontal flight, in steady flight as function of velocity (top), and in some maneuver flights (bottom).

rectilinear flight or in turn flight (bottom footprints). For the steady flights the plot of noise level versus velocity shows not only the dBA maximal values as previously but also the dB SEL level on centerline which should be homogeneous if the flights had been perfectly steady. For steady horizontal flights, we can notice that roughly the fastest is the quietest and the slowest the loudest (the strange noise footprint snapshot shape at 20 kts is due to excessive background noise on a lateral microphone). The trend of noise decrease with increasing speed, already observed for the dBA max values is even increased in dB SEL due to the corresponding variation of exposure time. Here we already get a guideline for pilots to fly silently: fly faster than 90 kts if possible and avoid staying a long time under 50 kts (for example when taxiing in ground effect or during only slightly decelerated descent with low angle and flare).

On the bottom part of Fig. 7, strong effects of maneuvering flight are shown on dBA noise snapshots. Note that the adopted microphone layout made it possible to capture the noise directivity during maneuver flights. Here the noise footprint is shown at a given reception time, but for the construction of directivity hemispheres [8] the data reduction is processed so that the noise directivity corresponds to a given emission time, i.e. to a given unsteady flight condition. Note that as well for the 2004 test matrix definition as for the noise simulation using the acquired data base, the helicopter noise emission was assumed to be mainly dependant on the main rotor advance ratio RmMu, its thrust coefficient RmCT and its tip path plane angle of attack PmAlpha. This choice is explained more in details in [6] and [8]. The influence of PmAlpha is here assessed by considering decelerated and accelerated examples. In the decelerated flight PmAlpha increases and reaches values also encountered in steady descent flights: 11 dBA max noise increase is observed at a given speed of 40 kts, in comparison to the level flight at constant 40 kts. The acceleration shown produces a 5 dBA max noise reduction at 65 kts. Examples of turn flights at 65 kts with 30 degree bank angle are also shown. Here the right turn (or more generally a turn towards the advancing blade side) does not bring much noise reduction whereas the left turn (towards retreating blade side) reduces the dBA max value by 5 dBA. An analysis presented in [6] led to opposite conclusions: the left turn was found to be louder than the right turn, also by comparing SEL footprints. The day of measurement of turn flights in 2004 was windy and there was turbulence. The noisiest dBA snapshot for the present right turn may result more from flight unsteadiness than from general tendencies of noise emission in turn. Indeed, after deeper examination of the 4 considered turn flights (the two mentioned in [6] and the two here) it was noticed that for all flights theta was between 0 and 3.5 deg at measurement time excepted for the present right turn for which theta reached 8 degrees. This seems to show that variations in PmAlpha (a higher theta leads to

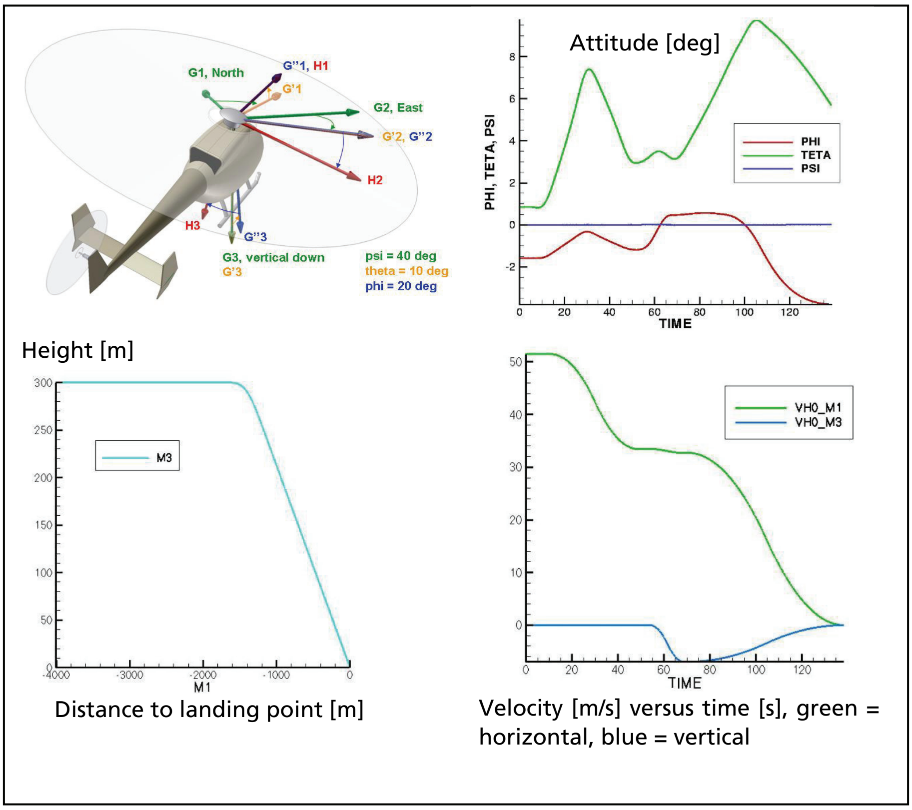

Fig. 8. Generic low noise flight procedure computed with HOST for flyability tests: horizontal deceleration, start of descent, descent (12 deg) at constant speed, decelerated descent and flare.

a higher PmAlpha in horizontal flight) have more influence than the direction of turn. The analysis of these unsteady turn flights should be revisited with the maneuver flight analysis technique shown in [8].

3. INVESTIGATION OF FLYABILITY LIMIT AND OF NOISE SENSITIVITY TO MAIN CONTROL PARAMETERS

In order to investigate the flyability of prescribed procedures, a generic procedure (Fig. 8) which contains the main expected piloting difficulties of low noise flight procedures was generated numerically. The path was described through way points and prescribed velocity at these points. Quintic splines (method explained in [8]) were used to generate a continuous flight procedure joining the way points and a HOST [11] inverse simulation was performed to find the flight conditions along this generic procedure.

The generic procedure contains following flight parts. A horizontal flight at 300 m height and 100 kts (51.4 m/s) is followed by a horizontal deceleration to 65 kts. The speed is stabilized and then (at 55 s) a conversion to descent flight at 65 kts and 12 deg slope is achieved. Between 70 s and 75 s the flight is steady (to allow pilots to rest a few seconds). Then the 12 deg descent path is followed in deceleration until landing. This generic procedure was tested in the EC135-FHS ground simulator (ground stands here for flight simulator on ground in order to avoid the confusion with the EC135-FHS itself which can be used as Flying Helicopter Simulator) in early 2007. The PAVE pilot assistant display (Fig. 9) providing prescribed velocity (left) and height (right) cues was used. The test pilots commented that the generic procedure was difficult to fly. They found that the test in the ground simulator was not enough representative for the real flight flight dynamics in order to conclude on the flyability: the real helicopter is easier to pilot than the simulator. The PAVE pilot assistant display was then tried in flight with the same generic procedure. The comparison of the prescribed and flown procedures are shown in Fig. 10. Height, airspeed, heading, and theta are plotted versus time (label every 20 s on the abscissa). We can see that velocity and height are accurately followed (excepted for the flare which was aborted) but that large changes in theta were applied to correct small discrepancies in velocity. These theta discrepancies/oscillations of 4-6 deg can result in much noise emission compared to the prescribed procedure as the main rotor angle of attack PmAlpha governs BVI occurrence. Pilots followed the cues they had as accurately as possible but as there was no theta cue, they were not aware of the large discrepancies in theta. In order to know if it is worthwhile to pay an accurate velocity control at the price of large theta oscillations, a noise sensitivity analysis was performed using 2004 flight test results.

Fig. 11 shows an analysis of steady flights noise levels. The abscissa is the True Air Speed. The ordinate is gammaA the aerodynamic glide slope. The contour levels show the maximum dBA level on ground when the helicopter is at 100 m height. We assume that a variation in theta of +n degrees produced by pilots in

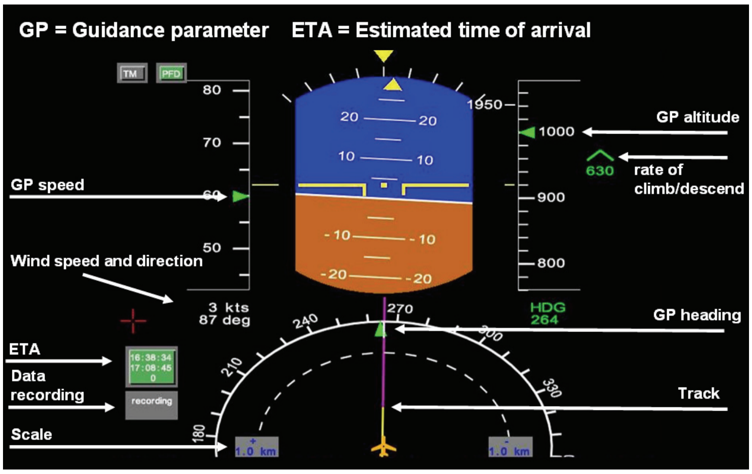

Fig. 9. PAVE Pilot Diplay [5], as used during the flyability tests of generic noise abatement procedures.

order to control the velocity on a given trajectory, has a similar effect on noise variation as a variation of –n degrees in gammaA for steady flights. This assumption relies on considering how PmAlpha varies with gammaA in steady flights and how it varies with theta during slight velocity corrections. For example during a flight at 55 kts and 10 deg slope (102 dBA max, bottom end of the vertical black arrow on Fig. 11), a pilot-induced theta-increase of 5 degrees would produce the same noise reduction as the difference between the stabilized 55 kts flights at gammaA = 10 deg and at gammaA = 10 – 5 = 5 deg (94 dBA max, top end of the arrow). We can thus estimate the noise sensitivity on theta to 8 dBA/5 deg = 1.6 dBA / deg. Within the accuracy in theta achieved in flight (Fig. 10) which is about 5 deg, variations of 8 dBA are possible. When we analyze the noise sensitivity to velocity (horizontal black arrow) we can read on Fig. 11 a sensitivity of up to 8 dBA max / 20 kts = 0.4 dBA / kt. The velocity accuracy achieved in flight of Fig. 10 is 4 kts, which represents variations of 1.6 dBA. For estimating the noise sensitivity to height we use the fact that the distance between the helicopter and the position on ground where the dBA max is perceived is proportional to the height. Then the spherical spreading law is used. For example a change in 8 dBA could here be achieved by a factor 2.5 in height. The height accuracy read in Fig. 10 is estimated to 5%, which represents a variation of 0.4 dBA. In summary the accuracies in theta, velocity and height produce respective uncertainties of 8 dBA, 1.6 dBA and 0.4 dBA. Consequently to fly acoustically accurately given flight procedures the weighting of the control parameters should be completely changed. The variable to follow the most accurately is theta, then the speed, and finally the height.

This has been taken into account in the further pilot display development. The projects time frames were so that the Friendcopter Display development could continue after the PAVE Display development was finished. Accordingly, the most advanced display to follow noise abatement procedures is now the Friendcopter Pilot Display, also developed at DLR (cooperation between acousticians, flight system specialists and pilots). The status reached by the Friendcopter Display for the 2008 validation flight tests is presented in Fig. 12. A tunnel in the sky interface was chosen as it is very intuitive for the pilot to follow a prescribed path in this way. The tunnel in the sky interface option was also possible on the final PAVE Display version and the present graphical layout concerning the tunnel, the sky and ground is very similar to what was reached and successfully tested in flight in PAVE. The consequence of the previous noise sensitivity analysis is the presence of a green theta target bar (plotted over the sky in the shown screen snapshot) and a 14 knots permitted velocity interval represented by a large target velocity bug on the velocity scale (on the left hand side). Theta was obtained from the HOST simulation of the entire flight procedure as explained in [8]. The height is considered accurate enough as long as the helicopter is in the tunnel whose section is 40 m high and 60 m wide. An additional height scale informs to the pilot about its height (air traffic control, height above ground). The bug

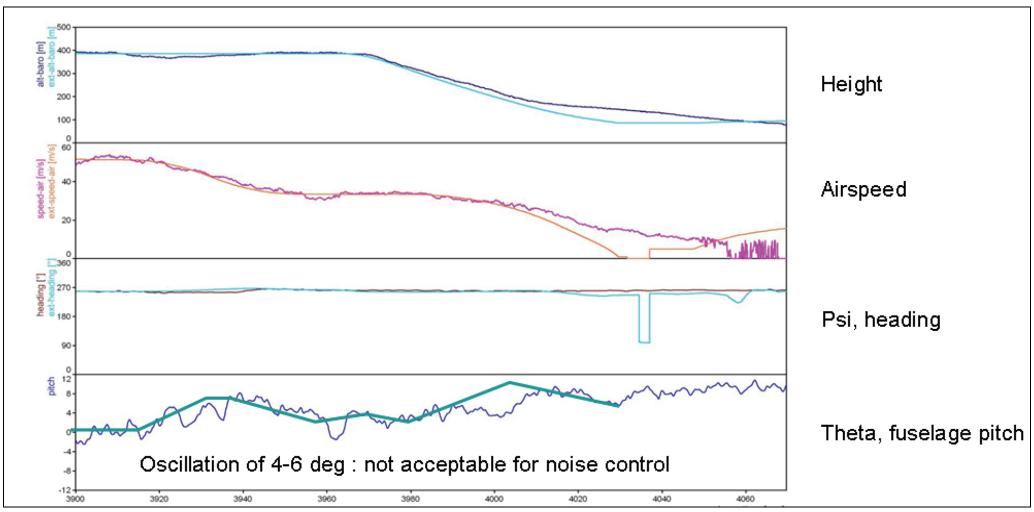

Fig. 10. Comparison between the prescribed parameters of the generic procedure and the one flown on EC135 using the PAVE pilot assistant that displays the prescribed velocity and altitude.

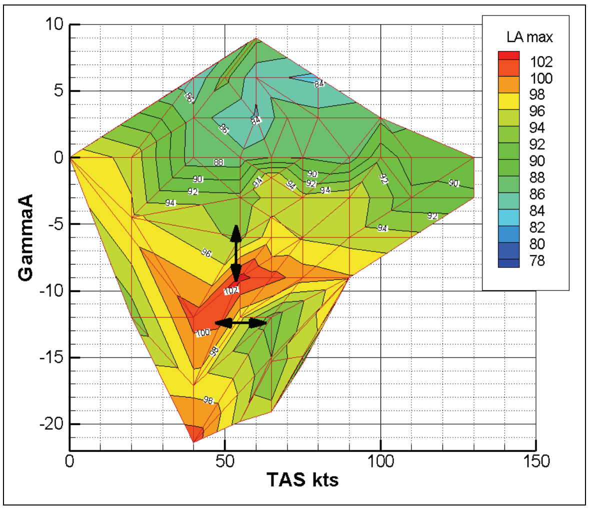

Fig. 11. dBA max on ground for steady EC135 flights when the helicopter is at 100m height.

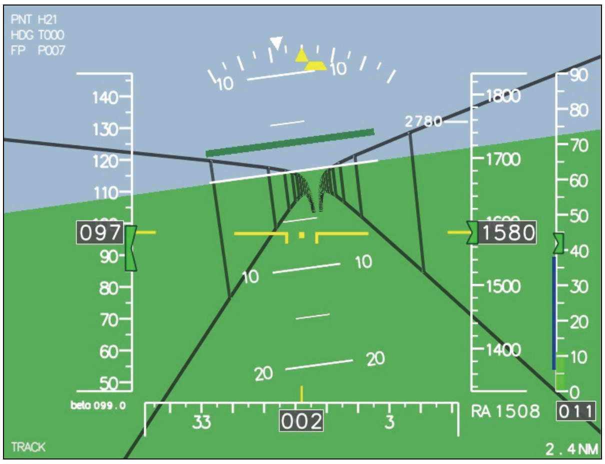

Fig. 12. Friendcopter Pilot Display developed at DLR for tests of noise abatement flight procedures.

on this altitude scale indicates the height of the middle of the tunnel sections. The pilots then controlled the helicopter to follow noise abatement procedures as follows: the cyclic stick is used to follow the target theta and to maintain the helicopter laterally in the tunnel. The collective stick is used to maintain the helicopter vertically in the tunnel. Keeping the helicopter in the tunnel is not sufficient. The tunnel should be followed smoothly, trying to keep the flight as parallel to the tunnel as possible in order to avoid lateral or vertical accelerations that change the main rotor thrust coefficient (RmCT).

In Fig. 13, an example of comparison between a prescribed optimized flight procedure and the corresponding flight piloted with the Friendcopter Pilot Display is shown. The height in black, theta in red and the velocity (with respect to ground) in green are given versus the horizontal distance HO_S1 of the rotor head center to the landing point. The thin lines represent the prescribed procedure and the thick ones the in-flight measured data. The pilot followed theta and the tunnel in the sky. We can notice that the oscillations in theta are reduced to 2-3 deg. It is not possible to reduce them much more because they are mainly due to turbulence. During days with more wind, theta presented higher oscillations, but still weaker than the ones shown in Fig. 10. These oscillations put aside, the pilot achieved to follow theta well, and hence indirectly the speed. Furthermore, the height discrepancies compared to the middle of the tunnel are weak.

Following the prescribed theta value does lead to the same velocity as in the simulated procedure only when the flight dynamic model in HOST corresponds to the helicopter at time of flight. Mass distribution changes, for example, can lead to equilibriums with other values of theta than in the simulation. Indeed, at speeds of 100 to 120 kts (flight part before descent), following the prescribed theta did not lead to the prescribed velocity: 10 kts difference were observed. However for the acoustically crucial descent part of the procedures, at speeds lower than 100 kts, following only the prescribed theta and the tunnel in the sky led indirectly to following correctly the prescribed velocity. No pilot-induced unwanted theta oscillations was observed.

Other aspects of flyability were also considered through a series of preliminary flight tests in Braunschweig (before the acoustic validation flight tests of 2008 at Magdeburg-Cochstedt Airport) and through the valuable pilot feed-back. This feed-back was taken into account in form of constraints in the procedure design. For example, a margin to autorotation was kept in order not to risk reaching autorotation that increases the main rotor rpm, which may damage the rotor. The flare, close to the ground, can not be piloted with display assistance, as the pilots must look outside for safety reasons (no head up display was used). Thus, the flare

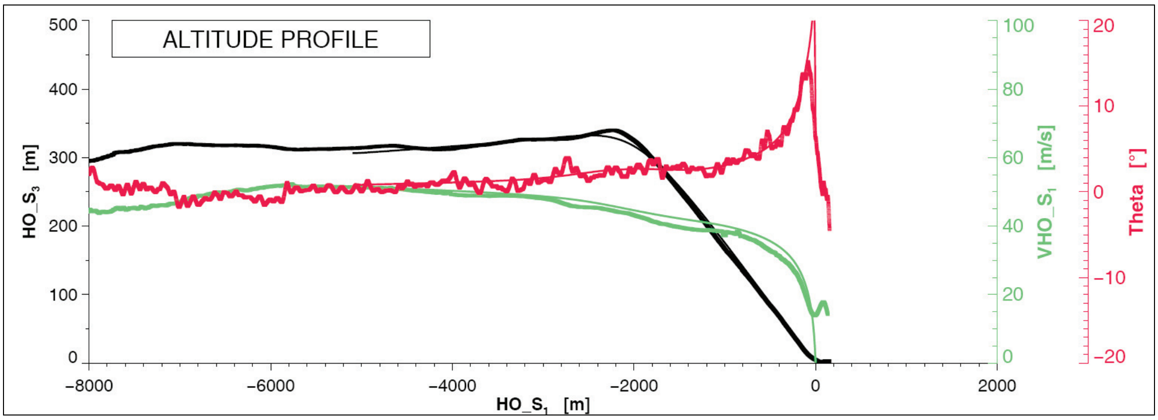

Fig. 13. Example of comparison between a prescribed optimized procedure (thin lines) and the corresponding flight piloted with the Friendcopter Display (pilot focus on theta and tunnel).

must be defined by instructions that pilots can follow without looking on a display. The noise abatement procedures have been designed for various wind conditions. Pilots then expressed limitations on landing approach directions, for example avoiding a tail wind component as this makes emergency procedures in case of engine failure close to the ground unsafe. Additionally, in order to avoid toppling-over risks when landing with non-zero velocity, the helicopter should be parallel to its velocity with respect to ground when coming close to the ground. In Section 2 it was shown that the fastest a flight is, the quietest it should be, at least for horizontal flights. As the velocity has an influence on the noise exposure duration, increasing the speed tends generally to reduce the SEL noise levels. Acoustically optimal landing approaches, simulated within the flight dynamics envelope of the helicopter (under various wind conditions) tend to consist of a very fast flight, with a transition in descent flight as late as possible, a steep and fast descent, followed by a strong deceleration just before landing. Even if the helicopter can theoretically fly such a procedure, the probability for pilots to overshoot the landing target is high in real flight. Indeed, with such procedures designed with no flyability margin, any difference between the real flight and the simulated one, as for example a weaker head wind component, or a too slow transition to descent, makes the landing approach fail, as there is no mean to recover the prescribed trajectory. The landing approach must then be repeated, which is of course far from an acoustically optimal solution. Moreover, flying such procedures stresses the pilots as they know that any slight discrepancy or adverse wind condition will make them overshoot the landing point. Therefore, the flare was extended horizontally (by 70 to 100 m) in the final procedure design, compared to the purely acoustically optimal procedure. With all these iterative improvements of the design, pilots succeeded in following the prescribed procedures during the 2008 acoustic validation flight tests. The landing point could be reached most of the time, which was not the case in the preliminary flights. It was also observed that the flyability of such unconventional landing approaches also increased with pilot-training.

4. TORQUE CONSIDERED AS A BVI GOVERNING CONTROL PARAMETER

Further considerations on how pilot work and how the available instruments in helicopter cockpits could help quiet flying, led to consider the engine torque display with attention.

Main rotor BVI can be avoided either by the convection of the vortices below the rotor plane, which is performed with a large collective pitch, or by their convection above the rotor plane, using a small or negative collective pitch value. Let us consider Pm the tip path plane coordinate system (as defined in the Friendcopter dictionary). Its unit vector Pm3 is perpendicular to the tip path plane and oriented towards the blade suction side. The flow velocity component along Pm3, averaged over the rotor disk, governs the vortex convection perpendicular to the rotor disk. It decreases (algebraically) when the collective pitch value (RmTheta0) increases at given thrust. At given thrust (RmThrust), the collective pitch (RmTheta0) and the required torque on the rotor shaft (RmTorque) are closely linked, as the collective pitch directly influences the projection of the aerodynamic force on each blade section in the rotor plane. When RmTheta increases RmTorque increases too. Consequently, at fixed RmThrust, the flow velocity component along Pm3 (averaged on the rotor disk) decreases when the torque increases.

When a given path has to be flown with another thrust (other helicopter mass), lets say a higher thrust, the collective pitch RmTheta0 has to be increased to achieve this thrust. Then the flow velocity component along Pm3 decreases. RmTorque increases because of the higher pitch (projection of blade section forces on the rotor plane) and because of the higher forces (for higher thrust) on each blade profile. Consequently a thrust increase at given path results in a torque increase and a decrease of the flow velocity component along Pm3, as in the case of Theta0 change at constant RmThrust.

The two previous paragraphs indicate qualitatively why it is expected that the main rotor torque and the velocity component of the flow perpendicular to the rotor disk, which governs BVI strength, are closely linked. The engine torque is closely linked to the main rotor torque as the engine and rotor rpm ratio is constant and as the main rotor is the dominant power consumer on the helicopter. Finally the engine torque is expected to be closely linked to the convection velocity component perpendicular to the rotor and consequently to govern BVI occurrence and strength. A complete theoretical demonstration and evaluation of the link between engine torque and BVI occurrence can become a time demanding task. The correlation between the engine torque and BVI noise is confirmed by an analysis of the PAVE 2004 test results, as shown hereafter.

In Fig. 14 the average dBA noise level on a segment of sphere of radius 300 m corresponding to the back-propagation from the 43 microphones are plotted as function of the horizontal airspeed and the engine torque at emission time (the same emission time for all microphones). The arithmetic averaging of dBA levels on the sphere segment was used. This noise level estimation has been made for instantaneous flight conditions selected on 3462 emission times during the flight test campaigns, when the helicopter was horizontally located at less than 150 m from the central microphone. The selected flight conditions are shown with black dots. The flight conditions cover as well maneuvering flights (in a vertical plane) as steady flights: the 3 parameters PmAlpha, RmMu, RmCT varied in a range of combinations that covers significantly the flight envelope necessary to design 2D arbitrary (but flyable) flight procedures. The torque values result from the HOST inverse computation of the test flights. The computed power of the main and tail rotor are considered to derive the total power. This total power is then divided by the engine rpm to get the engine torque. Then, this torque is divided by a nominal torque to get the engine torque ratio (variable indicated

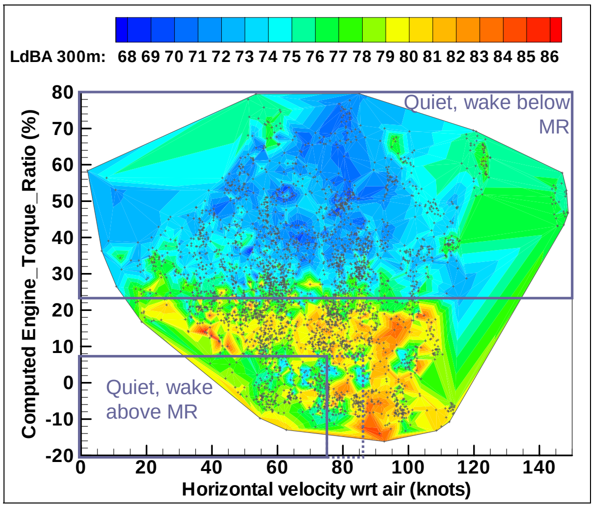

Fig. 14. Average dBA levels on a sphere of radius 300m, as measured in 2004, versus horizontal velocity and computed engine torque ratio. The black dots are the 3462 measured flight conditions.

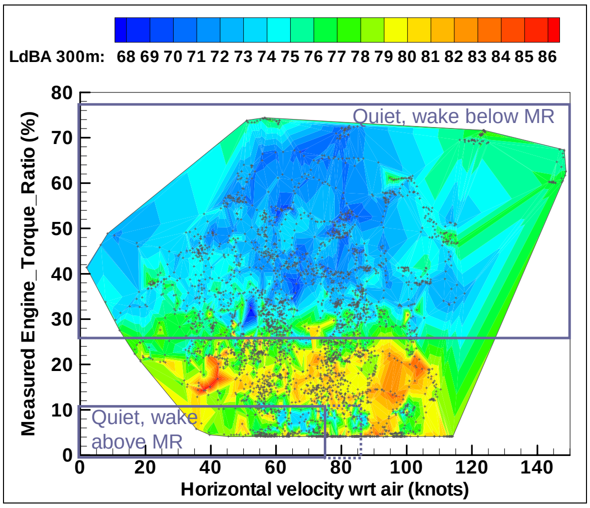

Fig. 15. Average dBA levels at 300 m versus horizontal airspeed and measured engine torque (never < 6%). The black dots are the 3462 measured flight conditions.

by an instrument on the control panel of nearly all helicopters). Note that the range of torque obtained is not realistic as it reaches negative values: this would mean that the power generated by autorotation would not have been totally consumed by the rotors. Thus the rotors should have increased their rpms, which was a configuration carefully avoided in flight because it is very dangerous. The torque computation was not accurate enough to reproduce the real flights. However it is assumed that the trends observed are nevertheless representative of their real flight.

It can be observed on Fig. 14 that there are quiet areas at high and at low torque. The high torque area limit is independent of airspeed in the range of measurement performed. Above 110 kts, nothing can be concluded on the limit as there was no measurement point for the expected noisy torque range (from 8 to 24%). The quiet area achieved with low torque is limited to speeds lower than 75 kts and partly to speeds lower than 85 kts. The noisier range completely at the bottom of the measured area is expected to be attributed to Fenestron noise.

In Fig. 15 the same plot as in Fig. 14 is proposed excepted that the engine torque ratio results from a in-flight torque measurement on the engines and the torque values achieved are exactly those indicated to the pilot. On the contrary to Fig. 14, no negative torque value are obtained. However no value is lower than 6%. It was recently checked in the preliminary flight tests, that even when reaching autorotation with a rpm slight increase (indicating that the rotor runs on free from the engine whose shaft rpm is stabilized by the FADEC system) the engine torque measure does not decrease below 6%. Therefore it is concluded that the engine torque is not really representative of rotor torque at low values. This is also indicated by the concentration of measurement points on the border 6% compared to the scattering of the same measurement point in Fig. 14. Therefore none of both previous torque evaluations is quantitatively satisfactory.

However the idea that BVI noise can be avoided with high torque over the whole velocity range and with low torque below 75 kts is nevertheless still considered and opens two possibilities:

1. Use of the torque display as a BVI indicator provided the torque limits in which BVI occur are given to the pilot.

2. Help the pilot to avoid BVI by avoiding a given torque range. As the engine torque value and the collective stick position are strongly linked it is relatively easy and fast to control the torque. The pilot has then the choice to fly with torque values above the noisy torque range or below. The first case corresponds to acceleration, high speed, or climb. The second case corresponds to or is close to autorotation. Autorotation can not only be achieved in steep descent but also in deceleration on path that do not need to be steep, as for example in flare.

In order to help the pilot to be aware of the noisy engine torque range, an extension of the torque display was proposed as in Fig. 16. A patent is pending for this concept. A variant of this concept consists in a velocity dependant indication of the torque range to avoid for flying quietly. Even if below 75 kts the noisy torque

Fig. 16. Torque display extended as noise indicator to the pilot.

range is constant it may be useful to have another indicated noisy torque range above 75 kts.

For the recent flight tests the torque indication and range to avoid was inserted on the right hand side of the Friendcopter Display as shown in Fig. 12. The current torque is indicated by a green vertical bar (not necessarily visible on the printed version of this paper as the printed green may be the same as for the background) and repeated digitally at the bottom of the scale. The green bug was meant to indicate the prescribed torque all along the path, but as this torque was computed as in Fig. 14 it was not reliable. However the noisy torque range was usable and indicated by the blue bar on the left hand side from the torque scale.

The optimization of flight procedures for noise minimization depends on helicopter mass and wind. Computing in advance such procedures implies that the procedure selected on board corresponds to the actual mass and actual wind. The actual wind can be estimated at helicopter height through the difference between GPS velocity and airspeed (speed of air relative to the helicopter). Then when the appropriate procedure is selected, a pilot display helping the pilot to follow accurately the procedure is required. The feasibility of this complete approach was demonstrated on EC135 in the validation flight tests mentioned in the next section.

Using the noise indication on torque is advantageous as the link between torque and noise seems independent of the helicopter mass. Indeed in Fig. 14 and Fig. 15 measurements with various masses were considered due to the fuel consumption during the test flights, which were performed from maximum take-off weight until almost empty tanks. If the noise would be dependant from the mass, additionally to the torque dependence, the quiet area on the figures would not appear. For the same reason, the noisy torque range concept is also valid in case of linear acceleration (controlled by collective pitch). The validity of the concept in presence of strong angular acceleration is not guaranteed as this kind of flights were not enough considered in the 2004 flight tests, and consequently in the previous figures. It is expected that angular acceleration affect much the noise emission as it needs cyclic pitch changes that change the azimuthal load distribution and consequently the azimuthal vortex intensity distribution at emission, and the distribution of the flow velocity component perpendicular to the rotor disk (influences the vortex paths). In the following sections only flights with weak angular accelerations are considered.

The limits of the torque range to avoid were set iteratively during the 2008 flight tests and preliminary tests. The range 8%-24% of Fig. 14 from the 2004 tests was considered as starting point. Subjective perceptions on ground were also considered. Finally the range that avoids both high measured ground noise levels and subjective annoyance was set from 6% and 55% as illustrated in Fig. 16. This different setting compared to the noisy area indicated in Fig. 14 or Fig. 15 can be due to the fact that the A weighting (for dBA) is not enough representative of human perception of impulsive noise and/or to the fact that the noise level averaging in all measured directions is not necessarily representative of the maximum noise perceived at given positions on the ground. All flights performed outside this final torque range were perceived as free of BVI noise.

5. PRESENTATION OF THE 2008 FLIGHT TEST SETUP

The 2008 flight tests aimed at validating the procedures optimized for various wind conditions (Friendcopter), and the procedures designed starting from the understanding of the physics (PAVE), as the torque concept of section 4. The same test setup was used for the PAVE and Friendcopter tests.

In order to quantify noise reductions reference procedures were defined and measured too. The optimized and reference procedures were flown using the pilot display (Fig. 12). The procedures based on torque avoidance were flown using the display only before the descent part. The descent flights were performed looking outside, the usual instruments and the torque display.

The Friendcopter teams working on EC130 [12], A109

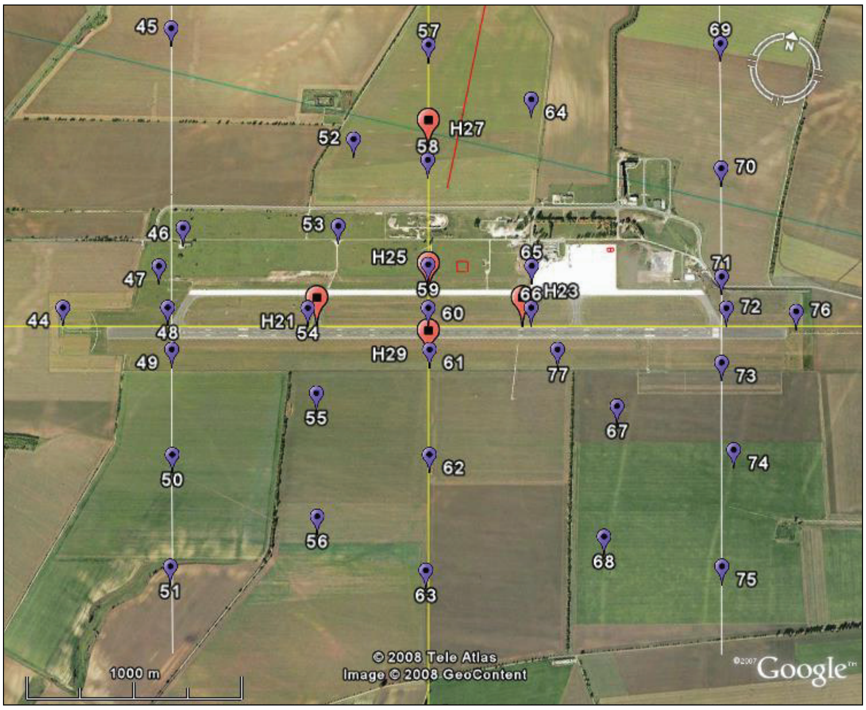

Fig. 17. Microphone (violet symbols) layout for the noise abatement flight procedure validations at Magdeburg-Cochstedt Airport in 2008. Yellow lines are flown paths and red symbols are landing points. The distance between Mics. 44 and 76 is 3350 m.

and EC135 in WP2 agreed that the noise minimization of the three helicopters must concern landing approaches whose common entry point is 5 km before the landing point, 1000 ft (305m) higher than it, and whose entry velocity is 100 kts. It was also agreed in Friendcopter to use SEL for noise quantification. All landing procedures considered are defined in a vertical plane (about 40 were defined and 159 flyovers performed).

For the EC135 flight tests in 2008 a total of 33 microphones were used with the same wireless measurement system as presented in [6]. As shown in the top view of the microphone layout at Magdeburg-Cochstedt Airport in Fig. 17, 31 microphones were scattered in a rectangle of 2510 m x 2475 m. Two additional microphones (Mics. 44 and 76) on the main flight axis extended the measurement length to 3350 m under the path when the directions of flight 77 degrees or 257 deg were used. 19 microphones were located in the fields outside the airport. In order to measure noise footprints of at least 5 km length corresponding to the length of the optimized landing approaches, the footprints are generated in 2 flyovers: the same procedure is flown twice above the microphone array but with a longitudinal shift. The shifted landing points outside the airport are shown in Fig. 18. For example when flying in direction 77 degrees, two landing points are used: first the point H23 and then the point H24. When flying in direction 257 the considered landing points are H21 and H22. The same process is used for the directions 167 deg and 347 deg. The effective flight directions were chosen at the last moment among those 4, depending on the wind direction (for example to avoid tail wind components). The noise contours shown in this paper consist of such assembled footprint as shown for example in Fig. 19. They are plotted in the coordinate system S. Its origin SO is the landing point. S1 is horizontal and oriented in the flight direction (during approach the S1 coordinate is negative). S3 is vertical upwards and S2 completes the right-handed system. Assembling the noise footprint leads, for the flight directions 77 deg, to a domain extend from -5100 m to + 1250 m along S1 and to a lateral extend S2 from -1276 m to + 1180 m. The assembled footprints concern up to 33 x 2 = 66 microphone positions in S. Fig. 19 shows the microphone positions in black dots and the triangulation mesh used for the noise footprint generation starting from the SEL noise levels on the microphones. 65 black dots are visible on the figure, and not 66, as the longitudinal shift of the landing points was defined in order to superimpose Microphone 44 (see Fig. 17) of the right hand side half footprint of Fig. 19 with Microphone 72 of the left hand side half footprint. In a same manner the Microphone 76 of the left hand side footprint is between Microphones 44 and 47 of the right hand side footprint. This enables to check that the two flights of the same procedure were acoustically similar. The number of microphone measurements really usable during the measurements can be less than 66, as no spare recorder was available in case of recorder malfunction. Unforeseeable transient background noise levels caused also some measurement limitations but usually only for the most lateral microphones, where the noise level to measure was very low. Therefore a sorting of the data has to be performed before processing them automatically. Note that the fact that the microphone layout used in 2008 is different from the one used in 2004 and reminded in Fig. 5 does not mean that the 2004 layout was found to be inappropriate. The goals of the measurements were different: acquisition of instantaneous detailed directivities during steady and unsteady flights on the one hand, and validation of complete landing procedures on the other hand. Each layout was adapted to its goal. The 2008 flight tests and their results will be better presented in a future publication.

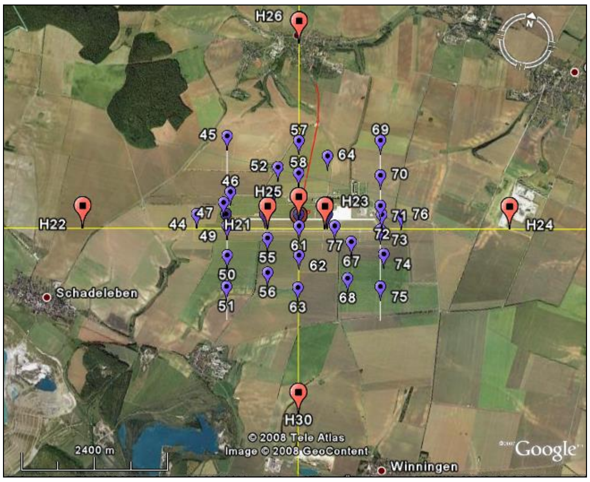

Fig. 18. View of the landing points far outside the airport: H22, H24, H26, H30.

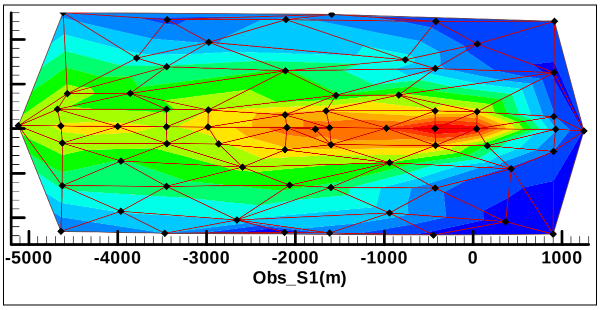

Fig. 19. Microphone position (66 black dots) and triangulation mesh (red lines), from an assembling of two single footprints resulting from flying twice the same procedure with a longitudinal shift.

6. ELIMINATION OF FENESTRON EXCESS NOISE USING SIDE SLIP

When the main rotor is operated close to autorotation in order to avoid BVI noise, the lateral force needed on the tail decreases and becomes zero in pure autorotation, as no main rotor shaft moment compensation is needed.

The fin of the EC135 as well as the small fins at the stabilizer tips are built with an angle of attack, in order to produce a lateral thrust in forward flight. This is illustrated on top part of Fig. 20. All forces are forces exerted by the air on the various components: F, M, R, and L are respectively the forces exerted on the Fenestron, the Middle fin, the Right fin and the Left fin at the tips of the stabilizer. This build-in incidence angles of the fins allow to reduce the thrust and hence the required power on the Fenestron and to continue the forward flight in case of Fenestron failure.

In case of forward (descending or decelerating) flight close to autorotation these fixed fins continue to produce a lateral thrust towards the advancing blade side (of the main rotor). The natural reaction of a pilot is to keep the helicopter in symmetric flight (with no side slip): he changes the Fenestron force direction in order to compensate the lateral force of the fins, as illustrated in the middle part of Fig. 20. This is made by acting on the pedals in order to change the Fenestron rotor blade pitch setting. The Fenestron produces then a lateral thrust towards the retreating main rotor blade side. Hence it has to work with reversed flow. In normal flow direction across the Fenestron, the flow crosses first the rotor and then the stator. In this case the rotor wake hits the stator blade with the crossing flow speed. The pressure fluctuations on the stator blades are limited as the blades do not turn. In case of reversed flow the flow crosses first the stator starting from the blade trailing edges and finishing on the blade leading edges, which probably produces a large wake, and crosses then the stator. In this case the stator wake hits the rotor blades with not only the crossing flow velocity but also with the rotor blade velocity. As the relative velocity between wake and blades is much higher than for normal flow the blade pressure fluctuations is much higher and quicker, and consequently the noise is much higher.

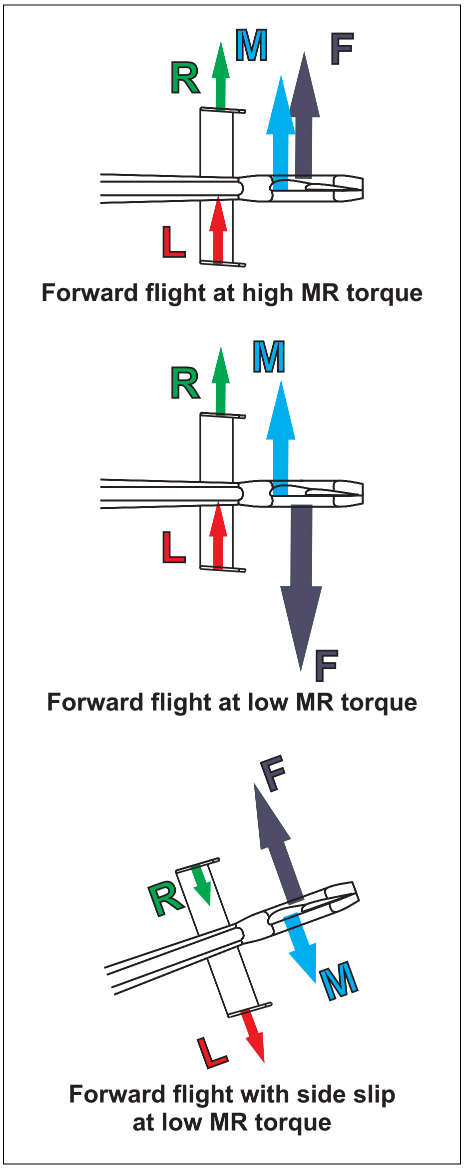

Fig. 20. Forces of the air on the vertical fins and on Fenestron: how the side-slip allows it not to reverse the Fenestron thrust and flow when the Main Rotor (MR) torque is low or zero.

This noisy situation has already been observed in flight tests in 2004. To avoid it there are two solutions.

1. Avoid using torque values too close to zero (autorotation) so that in flight with no side slip the Fenestron remains loaded in the normal direction (normal flow direction). This has been tried in the PAVE and Friendcopter Project noise abatement procedure design. However, in practice this solution suffers from lack of robustness. Indeed, the gap when reducing the torque, between the elimination of BVI noise and the appearance of Fenestron noise is very small and corresponds to 2 or 3 degrees in aerodynamic glide slope gammaA or rotor tip path plane angle PmAlpha for an 80 kts stabilized descent. In perfect calm air such an accuracy can be reached, but in current use turbulence can easily produce changes in PmAlpha of such and amplitude. Furthermore, if the followed procedure was not designed for exactly the same vertical wind-profile as the real conditions, the real gammaA obtained when following exactly the designed procedure differs also from the designed gammaA. The BVI region or the Fenestron excess noise region can then be reached even when prescribed procedures are followed accurately.
2. Fly with side slip when reducing the torque close to zero. This is illustrated on the bottom part of Fig. 20. The side slip results in inverted angles of attack of the fins and the Fenestron can produce a thrust in the same direction as for flights with high MR torque. The helicopter nose has to point towards the retreating blade side. This solution was considered in the flight tests.

As the EC135-FHS is equipped with velocity probes on a nose boom the side slip beta could be measured in

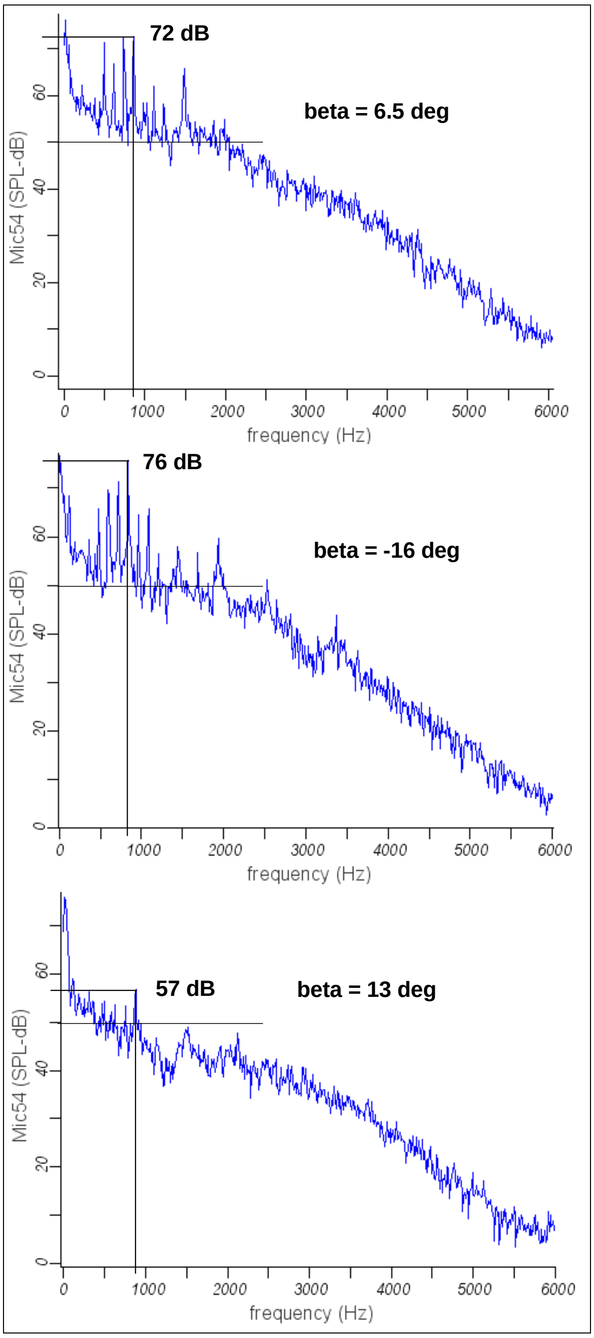

Fig. 21. Noise spectra at Microphone 54 for Procedure 11 flown in direction 347 towards H27, when the helicopter crosses the runway (stabilized descent), for 3 flights with different values of side-slip. The effect on Fenestron noise appears clearly.

flight and plotted on the pilot display. In order to check the Fenestron noise evolution versus side-slip, for low MR torque values, the procedure shown in Fig. 13 was flown 3 times with following prescribed side-slip settings during descent: 1) no side slip (beta = 0 deg), 2) with the nose turned 15 deg to the right (advancing blade side, beta = -15 deg) and 3) with the nose turned 15 deg to the left (retreating blade side, beta = 15 deg). Those flights were performed in direction 347 deg, towards the landing point H27 (see Fig. 17). Example of spectra recorded at Microphone 54 are shown in Fig. 21, for emission times corresponding to the crossing of the runway yellow axis. The helicopter height at

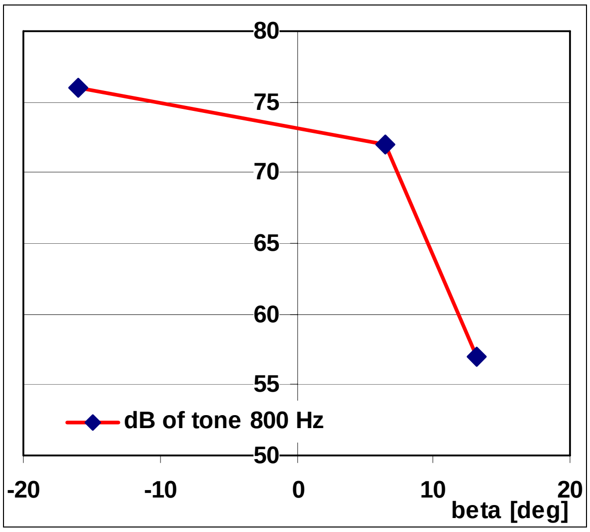

Fig. 22. Evolution of the sound pressure level of the Fenestron tone close to 800 Hz, in 80 kts descent flight at gammaA = - 15 deg, versus side-slip beta.

emission time was 162 m for the two first flights and 132 m for the last one. The S2 coordinate (lateral) of Microphone 54 is 550 m. The beta values reached at emission times were not exactly the prescribed ones (0, -15, + 15 deg) but 6.5 , -16 and 13 deg. The corresponding measured engine torque ratios were 5%, 16% and 5%. The first case, meant to be without side-slip, produces relative loud Fenestron noise and tones appear on the spectrum starting from 500 Hz, the highest tone being close to 800 Hz, with an level of 72 dB. The beta = -16 deg case produced an increase of the 4^{th} tone up to 76 dB. The Fenestron noise was perceived as very annoying. In the beta = 13 deg case the Fenestron noise could be reduced to become indiscernible to listeners, and on the spectrum, the tones have also nearly disappeared. The 800 Hz tone is decreased to 57 dB. On Fig. 22, the levels of the dominating 800 Hz tone are reminded versus beta. Compared to the interpolated solution of a flight with zero beta (73 dB) a side-slip of 13 degrees (nose towards the retreating blade side) produced a 16 dB reduction of the Fenestron tone noise (measure on the dominant tone).

The optimizations made in Friendcopter are based on the consideration of the RmMu, RmCt and PmAlpha. Beta was not considered as an additional noise parameter as it would have been too expensive in the 2004 tests to repeat all the flights for several values of beta. Beta investigations were made but unfortunately not close to autorotation. Therefore the optimization process uses the approach 1 above to reduce the noise. It automatically avoids going too close to autorotation in order to avoid Fenestron noise. In fact this avoidance could not entirely be achieved for real flights: in preliminary tests with wind from 5 to 10 kts the turbulence made the conditions vary so that BVI noise and Fenestron noise appeared alternatively. It was then decided to fly all optimized procedures with beta = 15 deg in the descent part of the procedures.

However pilot could not well stabilize the flight with this prescribed beta. For example in the flight mentioned above with beta = 13 deg, the side-slip oscillated at approximately 0.3 Hz with peak-to-peak amplitudes varying between 4 and 10 degrees. Pilots suspected the fin to stall and the flow to reattach alternatively. These beta oscillation also induced theta oscillation, resulting in a higher pilot workload to follow the procedures, in a non comfortable flight and in BVI noise apparitions.

Another solution was then proposed: It consists in not changing the Fenestron rotor blade pitch angle, when starting the descent flight and to keep this pitch until torque increase at flare. This is achieved by not changing the pedal positions, when decreasing the collective pitch to start the descent flight, and by keeping this pedal position fixed during the descent. This method appeared to be a flyable solution. The beta angle is unsteady at the begin of descent with slight oscillations but quickly converges to a quasi constant value. Remaining beta oscillations, the ones not due to torque or velocity changes are weaker than 3 degrees peak-to-peak. The resulting flight is a smooth descent without Fenestron noise excess and if the torque is low enough without BVI noise. The resulting beta is around 20 degrees and a phi (roll) angle of about 10 degrees is produced by the lateral thrust of the flow around the fuselage.

When coming to flare (Fig. 1), pilots must first increase the collective pitch (or torque) and then adjust the fuselage heading parallel to the path. If they first act on pedals to bring the heading in path direction and then pull the collective stick the noisy Fenestron condition can be reached, as even close to flare the main rotor torque can be very low.

The descent approach with side-slip, when flown without a display but just the torque control has the advantage to enlarge the view of the pilot. Indeed, for a pilot seating on the right hand side seat, a side slip flight with the nose turned on the left hand side, allows him to see in flight direction through the lateral window, which makes the view in steep angle possible, which is appreciated for steep descent flights.

7. BVI NOISE FREE AND FENESTRON NOISE FREE LANDING PROCEDURE FOR EC135

The definition of flyable noise abatement procedures was an iterative process involving design or optimization and a series of flight tests: preliminary flight tests in 2007 and 2008 in Braunschweig and validation flight tests in 2008 at Magdeburg-Cochstedt Airport. Starting from the output of Section 2, procedures were first designed by hand and simulated with HOST, focusing on the small slot of PmAlpha free of BVI noise and of Fenestron noise. For example, a procedure starting with a slight horizontal deceleration from 100 kts to 70 kts (assuming that the vortices remain below the main rotor), followed by a descent at 12,5 deg (assuming the vortices remain above the rotor) and a reduction of the slope simultaneously with a deceleration to flare was designed. It was first observed that the decelerated part did not allow to avoid BVI and the descent part was only quiet when no turbulent wind was blowing. Turbulence produced either BVI occurrence or Fenestron noise occurrence. When introducing the concept of flying with torque-range-avoidance, BVI free descent flights and flare could be achieved, but not necessarily with a quiet Fenestron.

The optimization process iterating automatically on the PAVE 2004 data base continued to converge to this PmAlpha slot between BVI noise and Fenestron noise, for various wind conditions. Indeed beta was not an optimization parameter, and no corresponding data for using it as such was available in the data base. The very steep descents (gammaA around -15 deg) or strong decelerations were not proposed as optimization output, and the full potential of BVI noise alleviation was not necessarily reached. In the preliminary tests of optimized flight procedures, occurrences of Fenestron noise and BVI occurrences were still present, particularly with turbulent wind.

Tests confirmed that side-slip could avoid Fenestron noise excess. It was then decided to fly all descent flights with side-slip, even the ones optimized in Friendcopter without side-slip simulation. Starting from that time, Fenestron noise was less and less a problem (it could be heard only in some short transient phases). This allowed exploring successfully very low torque approaches. In the meantime the optimization process with some additional way points as degrees of freedom also tend to avoid a medium torque range, choosing a high torque at the beginning of the procedure and then switching swiftly to a low torque. The high torque part of the optimized flights became a climb a soon as a constraint of maximum altitude of 1000 ft during the whole procedure was removed. The torque based approaches were then designed to begin with a similar climb.

We can here see that the systematic optimization approach (Friendcopter) and the design based on physics understanding (PAVE) were complementary and led finally to similar conclusions.

We now present some quantitative results for 3 flights measured at Cochstedt in 2008 and presented in Fig. 23. Here only some already available examples (not necessarily the bests) are shown to validate the described piloting concepts.

Fig. 23 (top) shows a procedure of Type 7 which was designed as a reference procedure. It is easy to fly as in connects smoothly the initial conditions and the landing. It crosses the noise certification descent flight conditions: 65 kts, 6 deg descent.

Fig. 23 (middle) shows a procedure optimized for zero wind. It is adapted ad hoc to allow for an extra 100 m for flare. It is called Procedure 46.

On the bottom of Fig. 23, a procedure based on the climb path of an optimized flight and a descent with low torque is presented. It is called of type 47.

All 3 flights were performed in the flight direction 77 deg (landing points H23 and H24 in Fig 18).

The left hand side of Fig. 23 shows measured noise footprints. The values of the SEL levels come from the online data reduction: each measurement unit computed and stored in real time dBA levels as

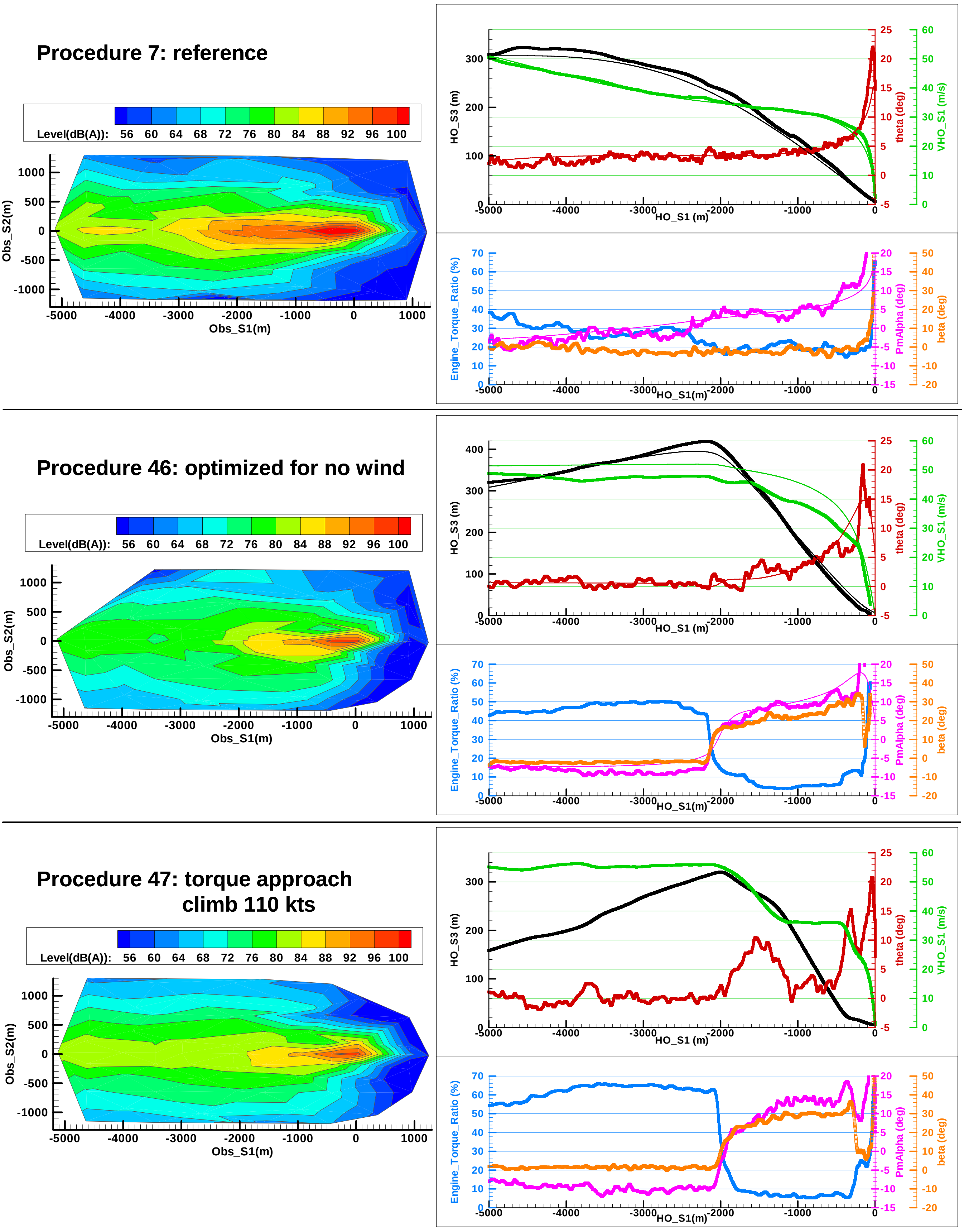

Fig. 23. Noise footprints in dB SEL and flight parameters of the reference procedure 7, the optimized procedure 46, and the torque approach procedure 47. The thin lines are the prescribed values of height (black), theta (red), velocity (green), PmAlpha (magenta) versus the position of the main rotor center HO on the flight axis S1. The thick lines are the corresponding measured values and the measured torque (blue) and beta (orange).

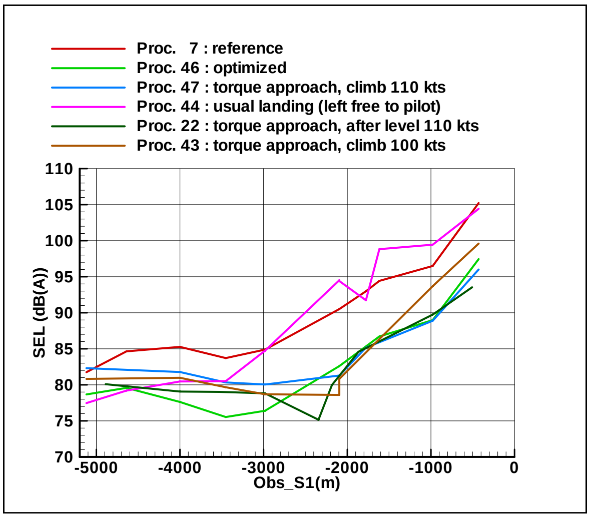

Fig. 24. SEL levels under the flight path of selected procedures.

function of time. These downloaded time histories were integrated offline in dB SEL.

The flight parameters of the 3 selected procedures are presented on the right hand side of Fig. 23, in two plots for each procedure. The top plot contains the pilot control parameters: the height (collective), theta (cyclic) and the speed. The bottom plot shows the measured engine torque ratio (as provided on the pilot instruments), PmAlpha, computed with an inverse HOST simulation fitting the real flight, and the measured beta. The thin lines are the prescribed values. The thick lines are the measured values.

The SEL evaluation on the centerline (vertical projection of the helicopter theoretical path on ground) of the 3 previously mentioned procedures is shown in Fig. 24 for an easier comparison of the procedures. The following procedures are added to Fig. 24.

Procedure 44, which is a so-called usual landing: the unique pilot constraint was to respect the initial condition and to reach the landing point. He was asked to land as usual.

Procedure 22 is like procedure 47 except that the climb is replaced by an horizontal flight at 325m and 110 kts.

Procedure 43 is like procedure 47 except that the climb part is at 100 kts.

It can be noticed in Fig. 24 that the usual landing is quieter than the reference procedure far from the landing point, and louder starting from 3 km to landing point. However, the level variation around 2 km distance, which is due to differences between the two flyovers (flown by the same pilot) necessary to get the 5 km long footprints, show that this usual landing approach can vary much from one approach to another.

On Fig. 23 we see clearly that the torque and PmAlpha vary smoothly on Proc. 7 whereas for Proc. 46 and 47 the torque remains first high and becomes then quickly low. PmAlpha varies similarly but in the opposite direction. Whereas on Proc. 47 the quick collective change results from an understanding of the physics, Proc. 46 results from the optimization. It can be noticed that beta reaches values up to 35 deg in Proc. 47. The increase in beta during the descent flight can be explained by the velocity reduction. Indeed, when the velocity decreases, the equilibrium between the constant Fenestron thrust and the lateral force on the fins needs an increase of the angle of attack of the fins.

Proc. 46 starts at 300 m with a climb. The noise reduction brought by the climb is clearly not due to the altitude increase as the noise level remains constant along Obs_S1 (between -5000 m and -3000 m) whereas the altitude increases.

We tried to remove the constraints of the initial altitude in the optimization. The result found was then a steeper climb beginning at lower altitude. Proc. 43 and Proc. 47 begin with the same climb slope as the optimized procedure. The Friendcopter pilot display was used by the pilots for this climb segment. However, at a certain distance from the landing point (set depending on the wind direction and strength), the collective stick is pushed downwards quickly and the descent is flown with no pilot display guidance.

The dBA max and the dB SEL only or mostly depend on the maximum noise measured, which occurs close to flyover. They do not account for lower noise values which can be annoying. The 2008 flight tests also indeed showed that the impulsive noise generated in forward direction is perceived during a long time until flyover and is unpleasant due to its impulsive character. The optimization process in dB SEL did not necessarily account for this phenomenon. Using other noise level units more appropriate to reproduce the psychoacoustic characteristics of human beings (i.e. also able to account for the long exposition of not so loud in dBA or SEL but nevertheless annoying noise) should be considered for the further data reduction and analysis or in future optimizations. To overcome this phenomenon, horizontal flyovers and climbs at 110 kts and 120 kts were tried (as suggested by the tendencies observed in Fig. 7). The subjective impression was that the forward impulsive noise was decreased at 110 kts horizontal flight compared to 100 kts and almost disappeared at 120 kts. When analyzing the evolution of the dBA level versus time on centerline during these horizontal flyovers (at maximum level time, 5 s before and 10 s before) following result is obtained.

dBA	-10 s	-5 s	0 s
110 kts	46	54	66
120 kts	45	52	70

It can be seen that even if the maximum noise level is higher at 120 kts, the dBA level is lower at 120 kts than at 110 kts, 5 s and 10 s before the time of maximum level. The levels 5 s before flyover are respectively 12 dBA and 18 dBA lower than the corresponding maximum levels and have therefore almost no influence on the SEL level evaluation. This underlines the interest of reconsidering the choice of the noise quantification method.

In climb (3 deg) the subjective noise decrease was as high at 110 kts as at 120 kts in level flight and the 120 kts climb flight did not bring a noticeable additional noise reduction. As the perceived impulsive noise did never increase with speed it is clear that it was not due to main rotor high speed impulsive noise but to main rotor BVI noise. Additionally, we can notice that the

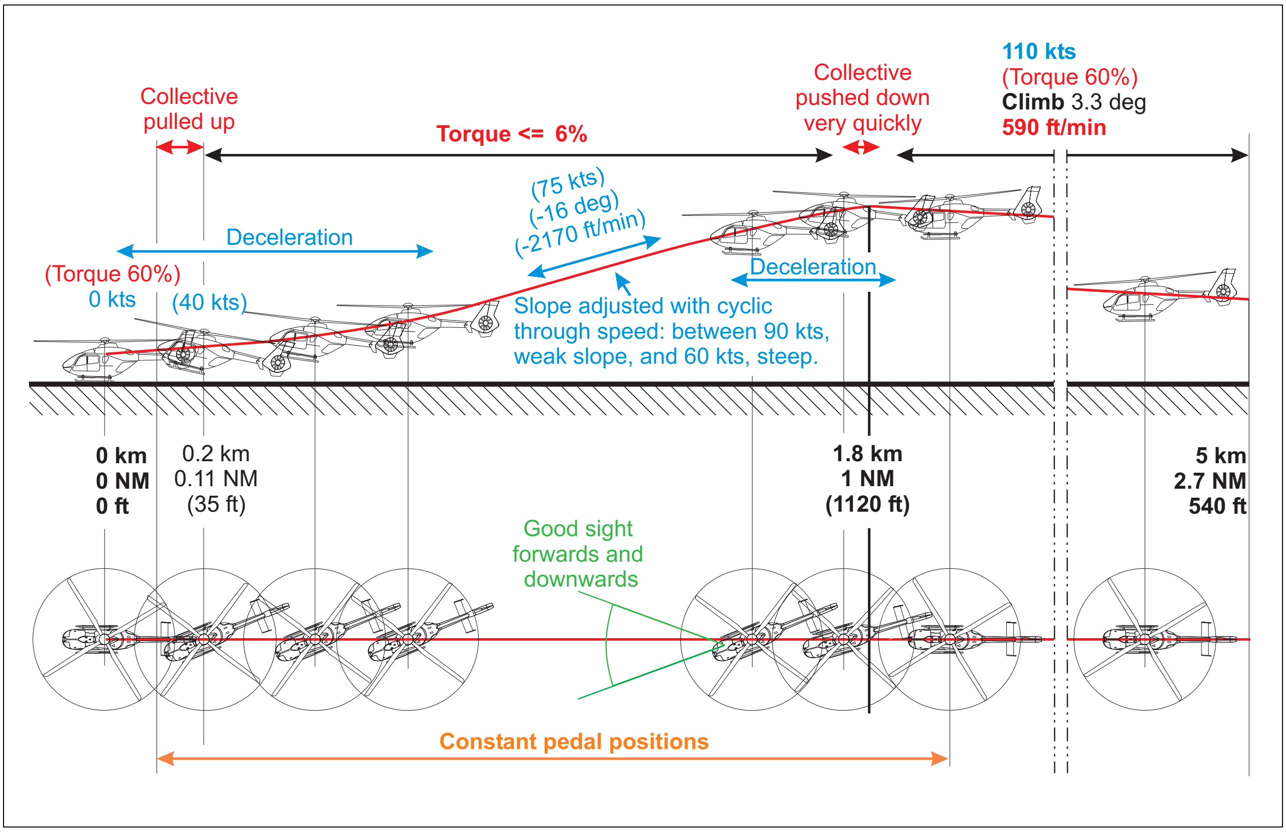

Fig. 25. Quiet landing procedure based on BVI noise avoidance through torque range avoidance and based on Fenestron excess noise avoidance through reverse flow avoidance by keeping the pedal positions. The slopes are respected in the figure.

perceived noise decrease was produced with torque increase (higher speed or climb).

According to the observations made, Proc. 47 was defined starting from Proc. 43 by increasing the speed during climb from 100 kts to 110 kts.

Even if in Fig. 24 it can be seen that Proc. 22 and Proc. 43 provide higher noise reductions between 5 km to 2 km before the landing point in terms of SEL levels, it is Proc. 47 which is considered the most interesting in terms of perceived noise reduction. The way to fly it is summarized hereafter as guideline to pilots.

Guideline to pilots for a quiet EC135 landing

How to perform a Proc. 47 like quiet landing approach of an EC135 is explained in Fig. 25. The values in brackets are for information and the values without brackets are conditions to follow. The red indications are for the collective stick, the blue ones for the cyclic stick and the orange ones for the pedals. This procedure can be flown without a special pilot display. Only two points need to be known: the entry point which is also the start of climb (5 km before landing point) and the start of descent point (1.8 km before the landing point). In presence of head wind component this distance may be advantageously reduced (for example to 1.6 km for head wind larger than 10 kts). These way-points can be programmed on an onboard GPS navigation system and the altitude red on altimeter. Therefore no sophisticated pilot display is necessary. However a display with a tunnel in the sky constitutes a valuable help to follow accurately the climb segment.

The procedure begins at 540 ft, with a 110 kts climb at 590 ft/min. When reaching the start of descent point, the pedals are maintained in constant position until shortly before landing (this avoids Fenestron noise), the collective stick is pushed down as quickly as possible (regarding comfort) to bring the torque to 6% (this start of descent is the only noisy part of the procedure, final landing put aside, and has therefore to be performed quickly) and theta is increased to 5 to 10 degrees to begin a deceleration. The RPM must be surveyed at low torque and the collective pitch increased if a RPM increase occurs. As the pedals are left in position, a side-slip of 20 to 30 deg appears and a resulting roll of 10 degrees. The side-slip avoids fenestron noise and additionally increases the sight forwards and downwards. During the whole descent close to or in autorotation, the pilot can adjust the airspeed between 90 kts and 60 kts (authorized range for autorotation) by changing theta with the cyclic stick, in order to adjust the slope, so that the landing point can be reached. At 90 kts, the slope is the weakest and at 60 kts, the steepest. The possibility to adjust the slope while remaining close to autorotation makes this procedure robust regarding wind variations. When the head-wind component is weaker than 5 kts, the recommended airspeed for the descent is 75 kts. The deceleration at the end of descent must be flown with low torque. The pedals can be moved again only after the torque recovery at the end of flare. The final landing maneuver should be performed quickly as well as the engine turning off, because the helicopter is loud at low speed and the only way to reduce the noise is to reduce its duration.

CONCLUSION

This article presents progress achieved in the design of noise abatement procedures for an EC135. The work has been conducted within PAVE and Friendcopter projects and has led to the following main results.

1 – The data documentation and reduction of former flight tests has been performed. The Friendcopter Dictionary of variables and coordinate systems has been written. It is used as common reference by Friendcopter cooperating partners for developments (HELENA) and flight tests. It is now open to public domain. It covers fields related to aircraft and rotorcraft aeroacoustics studies.

2 – The analysis of the test data from 2004 showed that, for 65 kts steady descent flights, there is only a slot between 12 and 15 deg descent slopes where both BVI noise and Fenestron noise can be avoided. Slow steady horizontal flights are loud and fast ones relatively quiet (reduction of 13 dB SEL between 20 kts and 130 kts). The comparison of steady horizontal flights with accelerated and decelerated ones showed respective noise variations of -5 dBA max and +11 dBA max on ground.

3 – Fflyability flight tests on generic procedures have shown that pilots can produce important variation of theta to control accurately the velocity. The analysis of the influence on noise of various control parameters showed that theta must be controlled accurately, the speed less, and the height not. This led to modifications in the pilot display developments and led to stabilized flights. Valuable feed-back from pilots improved the NAFP design process to guaranty better flyability.

4 – The engine torque ratio (displayed to pilots in almost all helicopters) was identified to be a parameter governing BVI noise. Iterative testing showed that the range 6% - 55% should be avoided in order to avoid BVI noise. This principle seems robust: except for a discontinuity at 75 kts, airspeed, mass and maneuvers have little influence on the noisy torque range.

5 – NAFP validation flight tests have been performed in 2008. Footprints larger than 5 km long and 2.4 km wide with 65 noise measurement points have been obtained (flying twice over 33 microphones).

6 – Flight tests showed that the Fenestron excess noise that appears when the main rotor works at very low torque (to avoid BVI) can be eliminated through side slip. Practically, the pedal positions should be maintained when decreasing the torque (with the collective stick).

7 – Some flight test results show that the simple principles mentioned above and the systematic footprint minimization performed in Friendcopter, allow reducing the noise of landing approaches by about 10 dB SEL. The best noise reductions occur generally close to the centerline (projection of path on ground), between 0.5 and 3.5 km before the landing point.

The experience gained during preliminary flight tests and validation flight tests allowed to provide guidelines to pilots on how to perform a quiet landing approach with an EC135, avoid BVI noise all the time except during 1 or 2 seconds (conversion to descent), and eliminating completely Fenestron excess noise. The quiet procedure can also be flown with the instruments commonly on helicopters and results in 8 to 10 dB SEL reduction between 0.5 km and 2.5 km from the landing point and also in a noticeable or impressive reduction of annoyance.

The flight test performed in 2008 will be more systematically analyzed. Origins of the engine torque differences in simulation and in flight should be investigated.

A way of separating the contributions of main rotor and tail rotor on total noise will be investigated using a computer program developed in Friendcopter. The noise characteristics should then be analyzed for both sources separately over the whole flight envelope (as tested in 2004), with emphasis on the not so well known Fenestron noise.

The methods being presented here are also applied to BO105. Optimized procedure have been designed and will be flight tested.

The NAFP optimization work wil continue in new projects with introduction of traffic management constraints and safety standard constraints, with investigation of non uniform sensitivity to noise on ground and 3D procedures. The pilot display will be further developped to be easily usable by non test pilots. Future works aim at applying the research results at operational level.

ACKNOWLEDGEMENTS

The works presented in this paper concerning on the one hand the dictionary of coordinate systems and variables and on the other hand the generation of the generic and optimized flight procedure were mainly performed in the European project Friendcopter WP2. All other works are part of the DLR internal project PAVE except the combined PAVE-Friendcopter flight tests of 2008. However the shown test results focus on PAVE results. This work has been conducted with the support of the European Union and of the German Ministry of Education and Research (project Friendcopter) and with the support of the German Ministry of Defense (project PAVE).

Special thanks go to the DLR test pilots Herbert Kistler and Uwe Göhmann and to the flight test engineer Waldemar Krebs (in 2008) for their competent, constructive an friendly participation especially by providing feed-back and suggestions concerning the flyability and safety aspects and suggestions for the pilot display development. The pilots are also thanked for their acceptance to explore unconventional ways to fly. The PAVE display development and use for the preliminary tests in Braunschweig was ensured by Thomas Lüken (also PAVE project leader) and the Friendcopter Display development was only possible thank to particular efforts and competences of Torsten Gerlach (coding and testing in simulator) and Joachim Götz (management). All authors but especially Anne le Duc, thank M. Adler, W. von Grünhagen, J. Götz (DLR) and B. Benoit, B. Claret (Eurocopter) for their always competent and friendly help with HOST. All colleagues and students helping for the acoustic measurements in Cochstedt are also thanked, particularly Michael Pott-Pollenske for the coordination and management of this large acoustic team (at least 22 persons).

Markus Lummer (development of the Bézier approach for automatic definition of continuous flights starting from way points and velocities at this points. Approach used in the optimization), Jianping Yin (nose boom velocity correction computation with UPM for the mesurement data correction), Thomas Lauke (introduction of an index and hyperlinks in the dictionary pdf document), Joël Brezillon (assistance in the Mode-Frontier Optimizer installation and use, expertise on optimization processes), Damiano Casalino (CIRA, mathematic formulation of flyabitlity constraints from the pilot handbook), Luis Meliveo (ANOTECC, contribution in the Delaunay 3D interpolation of flight conditions), Killian Meyer (preparation of microphones and cables, central computer survey and acoustic data back-up), Daniela Almoneit (online plots for flight procedures, noise level time history and noise footprints), Klaus Alvermann, Carl-Henrik Oertel and Hans-Peter Schwaneck (simulator and on board measurement systems of EC135), Kai Schwark (Maintenance of EC135), Carl Christoph Schoenwald and Rainer Holland (Telemetry for EC135-FHS), Robin Lantzsch (assistance for telemetry and preliminary simulator and flight tests), Thomas Wimmer (Flight Test Engineer in 2004), the University of Hannover with particularly Holger Shilke and Michael Theunsner for the weather measurement and forecast, Silke Buschmann (Managing Director of Mageburg-Cochstedt Airport), the airport employees - Bernhard Scheer, Axel Bertram, Norbert Henze -, the farmers - Ingbert Schulz, Helmut Höhne, Walter Taentzler, Peter Görtz, Steffen Schmidt, Manfred Unte - for their kind agreement for allowing access to and preparing their fields for noise measurements.

<u>Authors workshare</u>

Anne Le Duc (at DLR from fall 2004 to March 2007): start of the preparation of the automatic noise footprint computation using flight test data, investigation of trajectory constructions using quintic splines, adaptations on HOST scripts for inverse simulation, writing of a major part of the Friendcopter dictionary, structuration and development of the core of HEMISPHERE2, in particular development of the back propagation to construct hemispheres, contribution to the definition of netCDF files for the 2004 flight test results storage and use, introduction of first flyability constraints.

Frédéric Guntzer (at DLR since April 2007) : completion of HEMISPHERE2 (coding of forward propagation, of a reflexion model for homogeneous ground, of an atmosphere table model, implementation of microphone plate correction, 2D triangulation on spheres, improvement of computation speed), construction of the spheres database, scripting and completion of the computation chain for the simulation of arbitrary flights using a flight test data base, automatic correction of the nose boom velocity measurement, introduction of the simulation chain in an optimizer, installation with parallelization of the optimization loop on a PC cluster, contribution to the definition of netCDF files, completion of flyability constraint coding, run of the noise footprint minimization for various conditions.

Heino Buchholz: measured data verification, storage and conversion in netCDF files (flight condition data, acoustic pressure time history, acoustic spectra, and weather data), completion of the 2004 data with mass time history and correction of synchronization hardware errors, preparation of the 2008 tests: on-line data acquisition for on-line plots, management and maintenance of the whole autonomous acoustic unit system.

Pierre Spiegel: architecture of the aeroacoustic method employed in the PAVE and Friendcopter projects for the EC135, project leader for the helicopter NAFP development at DLR, flight test leader, definition of the microphone layouts, crew briefing and feed-back collecting, noise relevant specifications for the Friendcopter pilot display development (theta bar and torque), assistance of new engineers in the helicopter field, dictionary initializing by setting the rules and structure, contribution to dictionary definitions, definition of netCDF file content, contribution in flyability constraints definition with pilots, analysis of the noise sensitivity to the main parameters, idea of the correlation between torque and noise and of using the torque display as noise indicator and BVI avoidance tool, idea to use side slip to eliminate Fenestron noise excess, idea to use constant pedal position for that. Definition of the PAVE type of flight procedures.

REFERENCES

[1] Spiegel, P.; Buchholz, H. and Splettstoesser, W., "**The "RONAP" Aeroacoustic Flight Tests with a Highly Instrumented BO 105 Helicopter**", *American Helicopter Society 59th Annual Forum*, Phoenix, Arizona, May 2003.

[2] Rataj, J.; Bender, K. and Kohrs, R., "**A Helicopter Pilot Assistant System for Inflight Mission Planning**", *26th European Rotorcraft Forum*, The Hague, The Netherlands, September 2000.

[3] Rataj, J.; Bender, K. and Kohrs, R., "**Pilot Assistant for Approach and Departure**", *27th European Rotorcraft Forum*, Moscow, Russia, September 2001.

[4] Kohrs, R., "**Pilot assistant - the next generation helicopter cockpit**" *European Rotor & Rescue Magazin, joined with "Rotorblatt - das Helikopter Magazin"*, Vol. April 2004.

[5] Lüken, T. and Korn, B., "**PAVE: A Prototype of a Helicopter Pilot Assistant System**", *33th European Rotorcraft Forum*, Kazan, Russia, September 2007.

[6] Spiegel, P.; Buchholz, H. and Pott-Pollenske, M., "**Highly Instrumented BO105 and EC135-FHS Aeroacoustic Flight Tests including Maneuver Flights**", *American Helicopter Society 61st Annual Forum, Grapevine, TX, June 1-3, 2005.*

[7] Abellò, J. C. and George, A. R., "**Wake Displacement Modifications to Reduce Rotorcraft Blade-Vortex Interaction Noise**" *Journal of Aircraft*, Vol. 41, No. No. 2, March-April 2004, pp. 290-303.

[8] Le Duc, A.; Spiegel, P.; Guntzer, F.; Lummer, M.; Buchholz, H. and Götz, J., "**Simulation of Complete Helicopter Noise in Maneuver Flight using Aeroacoustic Flight Test Database**", *American Helicopter Society 64th Annual Forum and Technology Display, Montréal, Canada, April 26th - May 1st, 2008*.

[9] ISO 1151-1 Edition 4, "**Flight dynamics - Concepts, quantities and symbols - Part 1: Aircraft motion relative to the air**", International Organization for Standardization, 1998.

[10] ISO 1151-2 Edition 2, "**Flight dynamics - Concepts, quantities and symbols - Part 2: Motions of the aircraft and the atmosphere relative to the Earth**", International Organization for Standardization, 1985.

[11] Benoit, B.; Dequin, A.-M.; Kampa, K.; Gruenhagen, W.; Basset, P.-M. and Gimonet, B., "**HOST: A General Helicopter Simulation Tool for Germany and France**", *56th American Helicopter Society Annual Forum*, Virginia Beach, Virginia, USA, May 2000.

[12] Marze, H. J.; Gervais, M.; Martin, P. and Dupont, P., "**Acoustic Flight Test of the EC130 B4 in the Scope of the Friendcopter Project**", *33th European Rotorcraft Forum*, Kazan, Russia, September 2007.